View metadata, citation and similar papers at core.ac.uk

brought to you by CORE

provided by Louisiana State University

Louisiana State University

LSU Digital Commons

LSU Master's Theses | Graduate School

November 2019

Immune Gene Diversity and Populations Structure of Reticulated Flatwoods Salamander (Ambystoma bishopi)

Steven Tyler Williams
Louisiana State University and Agricultural and Mechanical College

Follow this and additional works at: https://digitalcommons.lsu.edu/gradschool_theses

 Part of the Biology Commons, Genetics Commons, Genomics Commons, Immunology and Infectious Disease Commons, and the Zoology Commons

Recommended Citation

Williams, Steven Tyler, "Immune Gene Diversity and Populations Structure of Reticulated Flatwoods Salamander (Ambystoma bishopi)" (2019). *LSU Master's Theses*. 5014.
https://digitalcommons.lsu.edu/gradschool_theses/5014

This Thesis is brought to you for free and open access by the Graduate School at LSU Digital Commons. It has been accepted for inclusion in LSU Master's Theses by an authorized graduate school editor of LSU Digital Commons. For more information, please contact gradetd@lsu.edu.

IMMUNE GENE DIVERSITY AND POPULATION STRUCTURE OF RETICULATED FLATWOODS SALAMANDER (*AMBYSTOMA BISHOPI*)

A Thesis

Submitted to the Graduate Faculty of the
Louisiana State University and
Agricultural and Mechanical College
in partial fulfillment of the
requirements for the degree of
Master of Science

in

The School of Renewable Natural Resources

by
Steven Tyler Williams
B.S., Virginia Polytechnic Institute and State University, 2012
December 2019

Acknowledgements

I would like to start by thanking my amazing fiancé Anna Perez-Umphrey who has encouraged me during this entire process. She has constantly supported me and provided emotional as well as academic support. This would not have been possible without her. I would also like to thank my parents and sisters for their support and encouragement which has sustained be throughout this project. Every member of the Taylor lab has helped me with advice and assistance multiple times and their comradery has been vital. I would also like to thank the RNR community and my hedgehog Piglet who has been my constant champion. Finally, Dr. Sabrina Taylor has been an amazing advisor and has skillfully guided me during my research and the development of my career, I cannot thank her enough.

This work would not be possible without the funding provided by Audubon Center for Research of Endangered Species (ACRES) grant. I am thankful to C. Rutt, A. Snider, A. Settlecowski, A. Bresnan, and T. Turner for extensive edits to this manuscript and my committee members, Dr. Kim Terrell and Dr. Chris Austin, for their support and helpful comments. I would like to thank Dr. J. Elbers for his tremendous bioinformatic assistance, without which I would have been lost. I am grateful to Dr. C. Haas and Dr. J. Roberts who have graciously shared these samples with me and to all the people who helped in sample acquisition: K. Jones, B. Rincon, V. Porter, C. Abeles, A. Farmer, P. Hill, L. Smith, R. Bilbow, J. de Silva, K. Erwin, B. Moore, J. Sandoval, E. Browning. I would like to recognize A. Wendt who extracted all of the DNA from samples collected on Eglin, Dr. M. Allender for providing a linearized *ranavirus* plasmid, and for sequencing assistance from Dr. S. Herke at the LSU genomics facility. Finally, I would like to acknowledge the Pennington Biomedical Research Center for the use of their facilities and Richard Carmouche whose expertise in genomic protocols was invaluable. Portions of this

research were conducted with high performance computational resources provided by the Louisiana Optical Network Infrastructure (http://www.loni.org). This project/work used Genomics core facilities that are supported in part by COBRE (NIH8 1P30GM118430-02) and NORC (NIH 2P30DK072476) center grants from the National Institutes of Health. This material is based upon work that is supported by the National Institute of Food and Agriculture, U.S. Department of Agriculture, McIntire Stennis program. Salamander samples were collected under Virginia Tech IACUC permit #16-100.

TABLE OF CONTENTS

Abstract

Reticulated flatwoods salamander (*Ambystoma bishopi*) populations began decreasing dramatically in the late 1900s. Contemporary populations are small, isolated, and may be susceptible to inbreeding and reduced adaptive potential because of low genetic variation. Genetic variation at immune genes is especially important as it influences disease susceptibility and adaptation to emerging infectious pathogens, a central conservation concern for declining amphibians. Connectivity between isolated populations is also vital to maintain genetic diversity and avoid inbreeding. I collected tissue samples from across the extant range of this salamander to examine genetic variation and population structure in: immune genes broadly (immunome), the major histocompatibility complex (MHC) class Iα and IIβ exons, as well as the mitochondrial control region. I also screened for *ranavirus*, a pathogen associated with amphibian declines worldwide. Overall, I found low MHC variation when compared to other amphibian species but mitochondrial diversity similar to other Ambystomatids. I also found moderate diversity in the immunome with possible gene duplication. I did not detect *ranavirus* at any site. MHC class Iα sequencing revealed only three highly similar alleles while MHC class IIβ sequencing found five alleles. However, unique variation still exists across this species' range with private alleles at several sites. I hypothesize that a combination of factors may have contributed to low MHC diversity, specifically, a historic disease outbreak and/or a population bottleneck. Ultimately, MHC data indicates that the reticulated flatwoods salamander is at an elevated risk from infectious diseases due to low levels of immunogenetic variation necessary to combat novel pathogens. Population structure and migration between major sites was calculated using all three genetic marker types (immunome, MHC, and mitochondria). Population structure for immunome and MHC data was low between major breeding sites, but mitochondrial structure was higher.

This pattern is indicative of male biased dispersal with females dispersing at a lower rate than males. Using program Migrate-N and BayesAss I calculated migration rates and found historic gene flow between salamander breeding sites. Since there is low population structure and historic migration between sites, I suggest human mediated dispersal of this species to re-establish gene flow and extirpated populations.

Chapter 1. General Introduction

The reticulated flatwoods salamander (RFS) is an endangered amphibian found in the southeastern United States. This species historically occurred in southern Georgia, Alabama, and the western panhandle of Florida but now is limited to only a few isolated breeding populations. The RFS follows similar patterns of amphibian declines worldwide: the two main drivers of these declines are habitat loss and the introduction of diseases, such as chytrid fungus and *ranavirus*. Immune genes are crucial in combating these pathogens and play a direct role in survival at the individual or population-level. Especially important is the major histocompatibility complex (MHC), which recognizes foreign antigens and triggers an immune response. Diversity at this region has been linked to survival following infection in amphibians. However, endangered species typically have lower genetic diversity and are at a greater risk of extinction from disease.

This thesis focuses on RFS immune genes to estimate genetic variation, population genetic structure, and migration between populations with the ultimate goal of informing future management and recovery of this species by maximizing genetic diversity and reestablishing historic gene flow. In the first chapter, MHC diversity is measured at two loci, MHC class Iα and IIβ, and is then compared to mitochondrial (mtDNA) diversity as well as MHC diversity as reported for 20 other amphibian species. Along with MHC sequencing, all RFS samples were screened for *ranavirus* infection. Estimates of diversity and disease prevalence can be used to assess the RFS's vulnerability to disease.

In the second chapter, next-generation sequencing techniques were used to isolate single nucleotide polymorphisms (SNPs) from a broad array of immune genes across the entire RFS

genome (the immunome). Diversity was measured at these SNPs and then these SNPs were used along with the MHC and mtDNA data from chapter 1 to estimate population structure and migration both within and between RFS breeding sites. Understanding patterns of migration and population structure at the landscape and local scale are necessary to determine the suitability of human mediated dispersal for the RFS.

Chapter 2. Depauperate Major Histocompatibility Complex Variation in the Endangered Reticulated Flatwoods Salamander (*Ambystoma bishopi*)

Introduction

The reticulated flatwoods salamander (RFS, *Ambystoma bishopi*) is a federally endangered species (ESA 2009) that occurs in fire-maintained longleaf pine (*Pinus palustris*) ecosystems (Palis 1996, Petranka 2010). Once a wide-ranging species, the RFS was locally abundant throughout the coastal plain of the southeastern United States and could be found in southern Alabama, western Georgia, and the panhandle of Florida west of the Apalachicola River (Palis 1996, Pauley et al. 2007, IUCN 2008). Over the last century, however, fire suppression, extensive land conversion, extensive droughts, and loss of longleaf pine habitat severely reduced and fragmented RFS populations (Frost 1993, Palis 1997, IUCN 2008, McIntyre et al. 2018). As a result, only twenty-two breeding sites could be identified when the RFS was listed as endangered in 2009. All breeding sites were restricted to Florida (n=20) and Georgia (n=2), with an estimated adult population size of just 10,000 individuals in 2009 (IUCN 2008, Pauly et al. 2007). Since that time, the number of known active breeding sites has declined from twenty-two to six (Farmer et al. 2016, O'Donnell et al. 2017, Semlitsch et al. 2017).

This severe decline in population size and breeding sites has likely caused a genetic bottleneck, which can lead to inbreeding and reduced genetic diversity. Inbreeding increases genome-wide homozygosity and may lead to inbreeding depression, causing reduced fecundity and survival. Genetic diversity is critical for long-term species persistence because it is the

foundation upon which natural selection acts, and it enables populations to adapt to changing environmental conditions (Frankham et al. 2002).

In particular, immune genes are crucial for species survival, as a diverse immune system is necessary to effectively combat a broad range of infections; without it, complex organisms would quickly succumb to disease. Moreover, disease represents the single greatest threat for many amphibian species and is a key factor in recent amphibian extinctions (McCallum 2007, Richmond et al. 2009). Chytrid fungi (*Batrachochytrium dentrobatidis* and *B. salamandrivorans*), in particular, have devastated populations of amphibians around the world (Berger et al. 1998, Martel et al. 2013, O'Hanlon et al. 2018), while *ranaviruses* (frog virus 3 and ambystoma tigrinum virus) are increasing in prevalence and beginning to spread globally (Chinchar 2002, Gray and Chinchar 2015).

In North America, *ranavirus* accounts for the most disease-related amphibian deaths each year (Greer et al. 2009), affecting both captive and wild populations (Johnson et al. 2008, Claytor et al. 2017). *Ranavirus* kills its host through a combination of lesions, abdominal swelling, and hemorrhaging (Gray and Chinchar 2015). Larval amphibians are the most susceptible to fatal infection and mass die-offs can devastate entire cohorts (Teacher et al. 2009). Some ambystomatid species, like the tiger salamander (*Ambystoma tigrinum*), can tolerate *ranavirus* prevalence (Greer et al. 2009) while others like the California tiger salamander (*Ambystoma californiense*) exhibit high mortality rates following experimental infection (Picco et al. 2007). This disease is spreading, and in recent years, amphibian deaths on five continents have been attributed to *ranavirus* (Marsh et al. 2002, Fox et al. 2006, Kik et al. 2010, Miller et al. 2011, Price et al. 2014). The incipient threat of disease in an interconnected world underscores

the importance of disease screening, biosecurity, and immune gene research for vulnerable species.

Major histocompatibility complex (MHC) immune genes are among the most important determinants of disease resistance in jawed vertebrates (Sommer 2005). This region is well studied and considered one of the most genetically diverse regions in the genome (Sommer 2005). MHC genes code for proteins found on the cell's membrane, which bind peptides derived from antigens and then present them for inspection to T-cells that in turn activate other components of the immune response (Bernatchez and Landry 2003). The MHC consists of two main classes: class I, which monitors intracellular fluid, and class II, which interacts with extracellular fluid. Class I proteins bind antigens found inside the cell and present them on the cell's surface to cytotoxic T-cells, which destroy infected cells (Alberts et al. 2015). These antigens usually derive from viruses or intracellular bacteria. Class II proteins present to and activate helper T-cells, which in turn activate B-cells, macrophages, and other immune cells. Class II proteins typically present antigens from extracellular bacteria and fungi (Alberts et al. 2015). Together these two classes of proteins combine to protect vertebrates against a diverse array of pathogens.

Genetic variation at MHC genes plays an important role in fighting infectious diseases. To date, most MHC related amphibian research has focused on anurans with less attention to caudates but show associations between diseases and MHC diversity. For instance specific MHC alleles have been associated with increased survival following exposure to chytrid fungus and *ranavirus* (Teacher et al. 2009, Savage et al. 2016, Savage and Zamudio 2016, Fu and Waldman 2017, Savage et al. 2018). Furthermore, MHC class IIβ heterozygosity correlates with increased survival in Chiricahua leopard frogs (*Lithobates chiricahuensis*) and lowland leopard frogs (*L.*

yavapaiensis) infected with chytrid fungus (Savage and Zamudio 2011, Savage et al. 2018). Similarly, wood frogs (*Rana sylvatica*) that are heterozygous at MHC class IIβ had a lower *ranavirus* infection intensity when compared to homozygotes (Savage et al. 2019). Because MHC diversity is important in combating pathogens, conserving that diversity will be a key component in countering the global species declines (Elbers and Taylor 2016, Savage et al. 2018).

In this study, we estimated MHC diversity in the RFS to investigate range-wide genetic variation. The control region of mitochondrial DNA was also sequenced to provide an additional estimate of genetic variation, but at a region that is unrelated to immune gene variation, and so unlikely to be affected by selection driven by disease. We also screened RFS for *ranavirus* infection to assess its occurrence across the range and to examine associations between immunogenetic variation and *ranavirus*, if present. Understanding the potential risk of exposure to *ranavirus* and the extent of immunogenetic diversity following bottlenecks will inform conservation efforts and management strategies for the RFS.

Methods

Sample Collection

Sampling occurred at five breeding sites across the extant range of the RFS (Figure 1.1). We used the breeding site definition laid out by the United States Fish and Wildlife Service, which considers any grouping of RFS ponds within 3.2km (2 miles) of each other as a single breeding site (USFWS 2015). Between 2011 and 2019, we collected samples at: East and West Eglin Air Force base (AFB), Florida (East: n = 147, West: n = 41); Escribano Point Wildlife

Management Area (WMA), Florida (*n* = 48); Garcon Point Water Management Area, Florida (*n* = 4); and Mayhaw WMA, Georgia (*n* = 5). Using sterilized scissors, tissue was taken either from the toes of adult salamanders caught in drift-fence funnel traps or from the tails of larvae captured during dipnet surveys. Both tissue types were stored in 95% ethanol at 4°C and DNA was extracted using a DNeasy kit (Qiagen) following the manufacturer's protocol.

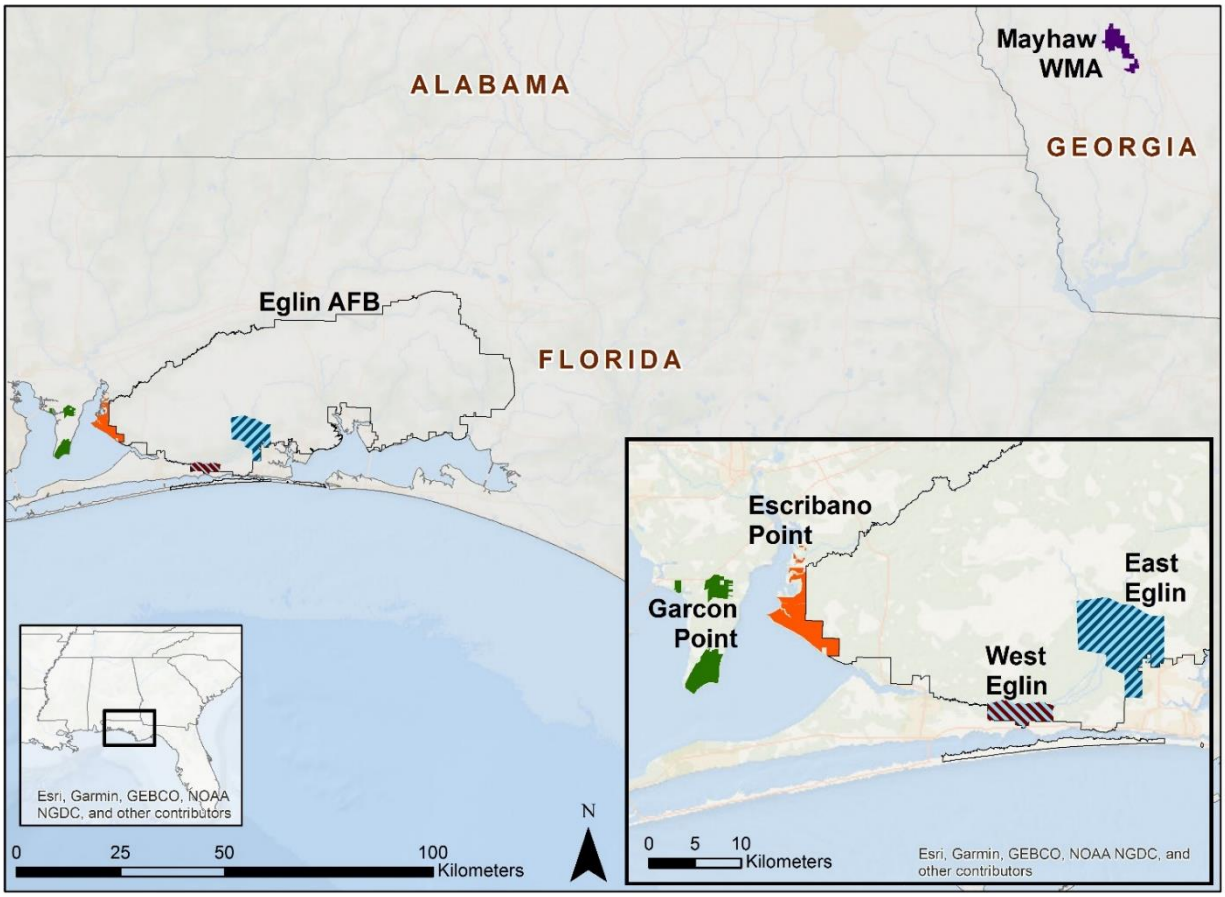

Figure 1.1. Map of breeding sites sampled for RFS from 2011 – 2019

Given the rarity of this species, sample sizes at each site were unbalanced, reflecting salamander abundance as well as sampling effort. The largest sample sizes came from Eglin AFB, where the RFS has been managed for more than ten years, including annual sampling of

both breeding sites. Escribano Point began managing RFS in 2014 at one breeding site, which was sampled comprehensively in 2018/2019. Garcon Point does not manage for RFS and so only one sampling event has been conducted to collect tissues at a single location, and since that time, the RFS has likely been extirpated from this site. RFS were recently discovered on Mayhaw WMA (2015), but because the extent of RFS occupancy is unknown at this site, only limited sampling at one location has been conducted to date.

DNA Amplification and Sequencing

We sequenced three loci: MHC class Iα exon 3, MHC class IIβ exon 2, and the mitochondrial control region (D-loop). MHC class Iα was amplified using primers P3S and P3AS as described in Sammut et al. (1999). PCRs were performed at a final volume of 20µl with concentrations of 1X PCR buffer, 3mM of $MgCl_2$, 4mM dNTPs, 6µM of each primer, 0.1µl of *Taq* polymerase (New England Labs, Ipswich MA), and 1.0µl of DNA template. The thermal profile consisted of an initial denaturation step of 30 s at 95 °C followed by 35 cycles of 95 °C for 30 s, 63 °C for 30 s, 68 °C for 30 s, and a final extension step of 68 °C for 5 min. Previously published primers (Bos and DeWoody 2005) did not amplify the MHC class IIβ locus in RFS, so we designed new primers using program Geneious v11.1.2 (Kearse et al. 2012, forward 5' GGATCTCCTTCTGGCTGTTC 3', reverse 5' CGAGTGCCGCWTTCTGAACG 3') based on published sequences for all ambystomatid species available in GenBank (AF209115, AF209117, DQ125478 - 80, KP408179 - 209). PCRs were performed as above except with a final concentration of 1mM of $MgCl_2$ and an annealing temperature of 60 °C. We also sequenced the mitochondrial D-loop, which has been used previously for genetic studies in the RFS (Pauley et

al. 2007). We amplified this region using primers THR and DL1 following Shaffer and McKnight (1997) and Pauley et al. (2007).

All PCR products were purified by combining 10µl product, 0.5 units Exonuclease I and 0.5 units shrimp alkaline phosphate (Affymetrix Inc) with nanopure water for a final reaction volume of 14µl followed by incubation at 37 °C for 30 min and then at 80 °C for 15 min. Purified PCR products were cycle sequenced in forward and reverse directions using 5x BigDye buffer (Applied Biosystems Inc), Big Dye v3.1, 10µM primer, 1.5µl purified PCR product, and nanopure water for a total reaction volume of 7.0µl. The thermal profile followed an initial step of 60s at 96°C followed by 24 cycles of 96°C for 10s, 50°C for 5s, 60°C 4 min. Cycle-sequenced product was purified with Sephadex G50 Fine (Sigma-Aldrich) and sequenced on an ABI 3130xl DNA analyzer at the LSU Genomics Facility (Baton Rouge, LA). All sequences were visualized, edited, and aligned using Geneious.

Pathogen Screening

RFS samples (*n*=249) were screened for *ranavirus* using primers 4 and 5 and the PCR protocol described in Mao et al. (1997). Primers 4 and 5 amplify a region of the major capsid protein and have reliably detected *ranavirus* infection in many amphibian species including the closely related tiger salamander (*Ambystoma tigrinum*: Picco et al. 2007, Greer et al. 2009) and more distantly related plethodontid salamanders (Blackburn et al. 2015). To confirm results, a random subsample (*n*=119) was re-tested with primers M151 and M152 (which amplify a different region of the major capsid protein gene) and the PCR protocol described in Marsh et al. (2002). Negative and positive controls were included with every PCR run. The negative control template consisted of nanopure water whereas the positive control was a 521bp fragment of

linearized *ranavirus* plasmid (Allender et al. 2013). All PCR product was run on 2% agarose gels, where the presence or absence of bands equal to the size of the positive control indicated the presence or absence of *ranavirus*.

Data Analysis

MHC variation was examined by using sequence data and by assigning each unique sequence an allele number (e.g. allele 01) to create genotype data. Estimates of nucleotide, allelic, and haplotype diversity were calculated in DNAsp v6 (Rozas et al. 2017). Observed and expected heterozygosity for MHC loci (Weir and Cockerham 1984) were estimated in GenePop v4.6 (Raymond and Rousset 1995, Rousset 2008). Each MHC locus was tested for Hardy-Weinberg Equilibrium (HWE) within each breeding site using GenePop v4.6. Significance values were adjusted using a sequential Bonferroni-adjusted alpha of 0.05 performed in R 3.5.1 (R Core Team 2018). Allelic richness, standardized to a minimum sample size of 4 individuals per population, was estimated with FSTAT v2.9.4 (Goudet, 2001). In order to translate sequences to amino acids and determine synonymous and non-synonymous nucleotide substitutions, the reading frame was selected by comparing the translation starting at nucleotide 1, 2, or 3. Each translation was inspected for stop codons (indicating an improper reading frame) in Geneious and compared to sequences of similar species published in GenBank. The d_N/d_S ratio was calculated and examined for evidence of selection using a *Z*-test with 5000 bootstraps to determine if $d_N = d_S$ using the Nei and Gojobori method with a Jukes-Cantor correction in MEGA X v10.0.5 (Kumar et al. 2018).

Results

At the MHC class Iα locus, we sequenced 190 individuals and observed three alleles (Table 1.1, Table 1.2) in a 243 bp region. These nucleotide sequences matched the MHC class Iα chain of the Mexican axolotl (*Ambystoma mexicanum*) with at least 90% similarity (NCBI BLAST algorithm, https://blast.ncbi.nlm.nih.gov/Blast.cgi, GenBank accession numbers U88185.1, U83137.1, and U83138.1). At the MHC class IIβ locus, we sequenced 93 individuals and observed five alleles (Table 1.1, Table 1.3) in a 160 bp region. These sequences matched with at least 90% similarity to the MHC class IIβ chain of both the Mexican axolotl and tiger salamander (NCBI BLAST algorithm, GenBank accession numbers KP408205.1, DQ125478.1, and DQ071905.1). We sequenced 682 bp of the mitochondrial D-loop in 238 individuals and observed nine haplotypes: seven were previously undescribed while two were 100% matches to haplotypes described by Pauley et al. (2007; Genbank accession numbers H2: EU517607.1 and H3: EU517606.1). One haplotype, H3, was found at all five breeding sites, whereas haplotypes H2 and H9 were shared among two sites each while seven haplotypes were private to a single breeding site.

Table 1.1. Genetic diversity estimates for MHC class Iα and IIβ in RFS.

Gene	Breeding Site	*n*	Alleles	Allelic Richnes	Private Alleles	H_O	H_E	Nucleotide Diversity (SD)
MHC Class Iα	Eastern Eglin	105	2	1.388	0	11	12.29	0.0005 (0.0001)
	Western Eglin	37	2	1.654	0	9	8.04	0.0009 (0.0002)
	All Eglin	142	2	1.46	0	20	20.44	0.0006 (0.0001)
	Escribano Point	39	3	2.835	1	23	25.08	0.0032 (0.0002)
	Mayhaw WMA	5	2	2	0	3	2.78	0.0023 (0.0003)
	Garcon Point	4	1	1	0	0	0	0 (0)
	Total	190	3	1.98	-	32	37.81	0.0013 (0.0001)
MHC Class IIβ	Eastern Eglin	29	3	2.253	0	11	15.72	0.0040 (0.0006)
	Western Eglin	26	3	2.509	0	9	13.51	0.0049 (0.0008)
	All Eglin	55	3	2.37	0	20	29.29	0.0044 (0.0005)
	Escribano Point	29	4	2.279	1	8	15.22	0.0041 (0.0006)
	Mayhaw WMA	5	2	2	0	3	2.33	0.0028 (0.0008)
	Garcon Point	4	2	2	0	1	1	0.0016 (0.0011)
	Total	93	5	2.471	-	32	49.95	0.0044 (0.0004)

Table 1.2. Amino acid sequences for MHC class Iα. Allele 1 and 3 are different by a single synonymous base pair substitution and occur on different breeding sites.

		1									10										20
	Allele 1	V	S	R	R	K	S	H	D	R	T	L	L	T	C	Y	A	Y	G	F	Y
	Allele 2	-	-	-	-	-	-	-	-	-	-	-	-	-	-	-	-	-	-	-	-
	Allele 3	-	-	-	-	-	-	-	-	-	-	-	-	-	-	-	-	-	-	-	-
		21									30										40
	Allele 1	P	R	E	I	E	V	K	W	I	R	S	G	V	E	M	P	L	E	W	S
	Allele 2	-	-	-	-	-	-	-	-	-	-	-	-	-	-	-	-	-	-	-	-
MHC	Allele 3	-	-	-	-	-	-	-	-	-	-	-	-	-	-	-	-	-	-	-	-
Class Iα		41									50										60
	Allele 1	Q	L	L	P	N	P	D	G	T	Y	Q	I	K	T	T	V	E	V	Q	E
	Allele 2	-	-	-	-	-	-	-	-	-	-	-	-	-	-	-	-	-	-	-	-
	Allele 3	-	-	-	-	-	-	-	-	-	-	-	-	-	-	-	-	-	-	-	-
		61									70										80
	Allele 1	G	H	K	E	K	M	Y	E	C	Q	V	E	H	S	S	L	P	E	T	A
	Allele 2	-	D	-	-	-	-	-	-	-	-	-	-	-	-	-	-	-	-	-	-
	Allele 3	-	-	-	-	-	-	-	-	-	-	-	-	-	-	-	-	-	-	-	-

		East Eglin	West Eglin	Escribano Point	Mayhaw WMA	Garcon Point
	Allele 1	0.941	0.882	0.474	0.500	1.000
Frequency	Allele 2	0.059	0.118	0.295	0.500	-
	Allele 3	-	-	0.231	-	-

Table 1.3. Amino acid sequences for MHC class IIβ.

		1																	18
	Allele 1	C	R	F	L	N	G	T	E	R	V	R	F	V	E	R	Y	S	Y
	Allele 2	-	-	-	-	-	-	-	-	R	-	-	-	-	-	-	-	-	-
	Allele 3	-	-	-	-	-	-	-	-	R	-	-	-	-	-	-	-	-	-
	Allele 4	-	-	-	-	-	-	-	-	R	-	-	-	-	-	-	-	-	-
	Allele 5	-	-	-	-	-	-	-	-	Q	-	-	-	-	-	-	-	-	-
		19																	36
	Allele 1	N	Q	Q	Q	L	L	H	F	Y	S	E	K	G	V	Y	E	A	D
	Allele 2	-	-	-	-	L	-	-	-	-	-	-	-	-	-	F	-	-	-
MHC	Allele 3	-	-	-	-	V	-	-	-	-	-	-	-	-	-	Y	-	-	-
Class IIβ	Allele 4	-	-	-	-	V	-	-	-	-	-	-	-	-	-	F	-	-	-
	Allele 5	-	-	-	-	L	-	-	-	-	-	-	-	-	-	Y	-	-	-
		37															52		
	Allele 1	D	L	L	G	V	P	D	A	Q	Y	W	N	S	Q	K	E		
	Allele 2	-	-	-	-	-	-	-	-	-	-	-	-	-	-	-	-		
	Allele 3	-	-	-	-	-	-	-	-	-	-	-	-	-	-	-	-		
	Allele 4	-	-	-	-	-	-	-	-	-	-	-	-	-	-	-	-		
	Allele 5	-	-	-	-	-	-	-	-	-	-	-	-	-	-	-	-		

		East Eglin	West Eglin	Escribano Point	Mayhaw WMA	Garcon Point
	Allele 1	0.483	0.404	0.483	-	-
	Allele 2	0.483	0.519	0.483	0.700	0.875
Frequency	Allele 3	0.034	0.077	0.017	-	-
	Allele 4	-	-	0.017	-	-
	Allele 5	-	-	-	0.300	0.125

For each MHC locus, a maximum of two alleles was recovered in every individual, indicating that pseudogenes and gene duplication were absent, as previously demonstrated with other ambystomatid MHC primers (Sammut et al. 1997, Bos and DeWoody 2005, Tracy et al. 2015). For MHC class Iα, only a single reading frame (beginning with nucleotide 2) produced an amino acid sequence with no stop codons. MHC class IIβ had two reading frames that did not produce stop codons (starting with nucleotide 2 or 3), but when the sequence was compared to the same region of the tiger salamander (DQ125478.1, and DQ071905.1), only reading frame 3 produced an amino acid sequence that did not contain a stop codon in either species. All further analyses were conducted using reading frame 2 for MHC class Iα and reading frame 3 for MHC class IIβ.

The d_N/d_S ratio did not differ from neutral expectations at either MHC locus, indicating no evidence for selection (MHC class Iα Z = -0.24, p= 0.81; MHC class IIβ test statistic = 0.55, p= 0.60). After Bonferroni correction, all breeding sites were in Hardy-Weinberg equilibrium except at Escribano Point for the MHC class IIβ locus (X^2 = 16.9, p = 0.03).

Eglin AFB as a whole (combining the East and West sites), had the highest levels of allelic richness, heterozygosity, and nucleotide diversity for the MHC class IIβ (Table 1.1), as well as the greatest number of haplotypes, highest nucleotide diversity, and greatest number of private haplotypes at the mtDNA D-loop (Table 1.4). In contrast, Eglin had lower MHC class Iα nucleotide diversity and allelic richness than all other sites except Garcon Point. Escribano Point exhibited the highest MHC class Iα nucleotide diversity and allelic richness. Escribano Point also was the only site to exhibit private MHC alleles, at both loci.

Table 1.4. Genetic diversity estimates for mitochondrial D-loop in RFS.

Breeding Site	*n*	Haplotypes	Private Haplotypes	Nucleotide Diversity (SD)	Haplotype Diversity (Variance)
East Eglin	144	5	4	0.0012 (0.0001)	0.594 (0.0010)
West Eglin	40	3	2	0.0021 (0.0003)	0.488 (0.0051)
All Eglin	184	7	5	0.0019 (0.0001)	0.679 (0.0007)
Escribano Point	46	3	1	0.0011 (0.0001)	0.645 (0.0012)
Mayhaw WMA	5	2	0	0.0006 (0.0004)	0.400 (0.0563)
Garcon Point	3	2	0	0.0001 (0.0005)	0.667 (0.0988)
Total	238	9	-	0.0019 (0.0001)	0.697 (0.0007)

Mayhaw WMA had intermediate levels of nucleotide diversity at both MHC loci. It also had very low levels of mtDNA haplotype and nucleotide diversity. Garcon Point was the least diverse site and exhibited low nucleotide diversity and heterozygosity at both MHC loci and mtDNA. Although Garcon Point and Mayhaw WMA did not have any private alleles, they did share a unique MHC class IIβ allele that was not found on Eglin AFB or Escribano Point (Table 1.4).

We did not detect *ranavirus* in any RFS samples, during any year, with either protocol, a result that is in accordance with records from the United States Geological Service wildlife health center database (https://www.usgs.gov/centers/nwhc/data-tools), which had no reports of *ranavirus* for either the RFS or the Frosted Flatwoods Salamander (*Ambystoma cingulatum*) in the last 100 years. Lack of detection in our samples was probably not the result of amplification issues: during every screening, the positive control amplified *ranavirus* DNA while the negative control never produced amplified product. However, other factors could have negatively

impacted our ability to identify virus, as *ranavirus* has been detected at low concentrations on Eglin with qPCR in other amphibian species (Dr. Carola Haas, personal comm.). Tissue type may have been a factor: although Greer et al. 2009 successfully used tail clips to detect *ranavirus*, other tissues like spleen harbor more viral DNA and may have returned different results. *Ranavirus* can also occur in pulse events, therefore its occurrence can vary widely from year to year (Gray and Chincar 2015), and it is possible that samples were collected during a period of little *ranavirus* activity. However, it is also possible that *ranavirus* really was absent as the nature of RFS wetlands might reduce the presence of disease. RFS ponds are dry for most of the year and the basins are burned with some regularity. If dry conditions and fire are inhospitable to *ranavirus*, and the absence of amphibian hosts during the summer month disrupts continuity of disease, it may not be surprising that we did not detect *ranavirus*.

Discussion

The MHC class Iα and IIβ diversity we observed for RFS was lower than levels observed in many other amphibians (Table 1.5), including species that have experienced severe population declines, such as the southern corrobree frog (*Pseudophryne corroboree)*, Mexican axolotl, and Chinese giant salamander (*Andrias davidianus)* (Zhu et al. 2014, Kosch et al. 2017). It is, however, difficult to make direct comparisons of MHC diversity between amphibians because, unlike many other vertebrates, most frogs and some salamanders have MHC pseudogenes and gene duplications (i.e. multiple loci) at MHC genes (Sammut et al. 1997, Bos and DeWoody 2005, Kiemnec-Tyburczy et al. 2012, Zhao et al. 2013, Tracy et al. 2015, Kosch et al. 2017). Nevertheless, RFS exhibits comparatively depauperate MHC class Iα diversity with few alleles

and low nucleotide diversity (Table 1.5), although, some species do show equivalent levels of MHC class IIβ diversity. For example, the mountain stream salamander (*Ambystoma altamirani*), plateau tiger salamander (*Ambystoma velasci*), and Chiricahua leopard frog all have five or fewer alleles and the mountain stream salamander also has similarly low nucleotide diversity. These three species have all experienced recent and dramatic population declines, caused mostly by extensive habitat loss for the salamanders, and chytrid fungus for the Chiricahua leopard frog.

Low levels of MHC diversity may have been caused by the documented population declines in RFS (this is supported by microsatellite data, indicating that a bottleneck has occurred on Eglin AFB (Wendt 2017)) and perhaps selection caused by previous exposure to disease. Population declines alone do not typically reduce MHC diversity to the extent observed in RFS. For example, the San Nicolas island fox (*Urocyon littoralis dickeyi*), Peary caribou (*Rangifer tarandus pearyi*), Chinese giant salamander, and the Lake Patzcuaro salamander (*Ambystoma dumerilii*) all retained more MHC alleles than observed in RFS despite population bottlenecks of similar intensity (Aguilar et al. 2004, Taylor et al. 2012, Tracy et al. 2015). Although these species may have had historically larger effective population sizes (and therefore greater diversity), comparisons of the relative loss of diversity among marker types is also suggestive. For example, genetic diversity as estimated with microsatellite data (H_E, H_O, AR) for RFS on Eglin AFB was comparable to other amphibian species (Wendt 2017), but MHC diversity was often much lower in RFS than in other amphibian species (Table 1.5). This pattern also holds for mitochondrial diversity: RFS mitochondrial diversity was similar to other ambystomatid species (Church et al. 2003, Zamudio and Savage 2003), whereas MHC diversity was lower. Similarly, the Chiricahua leopard frog, which experienced a bottleneck caused in part by disease pressure, apparently lost much of its MHC diversity but retained mitochondrial

diversity (Savage et al. 2018). Thus, a population bottleneck in combination with an undetected historical disease outbreak in RFS could have reduced MHC diversity but not mitochondrial diversity to the same extent. Low MHC diversity suggests that the RFS is at an elevated risk from infectious diseases, as it lacks the broad spectrum of alleles necessary to combat novel pathogens (Savage et al. 2019). *Ranavirus* is spread easily, and if the few remaining RFS breeding sites were exposed to this virus or any other amphibian pathogen, it could negatively impact population size, cause local extirpations, or even drive the species to extinction.

Biosecurity measures to prevent the spread of disease, such as equipment bleaching and ethanol decontamination, are currently in place at most breeding sites; however, application is not uniform and disease screening is irregular. Although we did not detect *ranavirus* in RFS, it is a highly virulent disease, and consequently, is one of only two reportable amphibian pathogens in the United States. Given the elevated risk of disease due to low immunogenetic variation, continued disease monitoring and proper biosecurity measures should be implemented at all sites to minimize future exposure to novel pathogens.

Despite low levels of genetic diversity, private alleles still exist across the extant range of the RFS. In particular, MHC IIβ allele 5 was found only at Garcon Point and Mayhaw. In spite of their smaller population sizes, these sites still harbor genetic variation, which contributes meaningfully to the overall diversity at that locus. In contrast, mitochondrial diversity was unevenly distributed across the breeding sites. Eglin AFB as a whole accounts for more than half of the recovered haplotypes, five of which were private, although the large sample size at Eglin AFB may explain higher levels of diversity than that observed at other sites. Nevertheless, no one location contains all remaining diversity and thus each extant breeding site retains high conservation value.

Table 1.5. Published MHC class Iα and IIβ variation in amphibian species. NR indicates that the metric was not reported.

Locus	Species	Sample Size	Number of Alleles	Nucleotide Diversity	IUCN Conservation Status	Citation
MHC class Iα	Reticulated Flatwoods Salamander (*A. bishopi*)	190	3	0.001	Vunerable	This study
	Chinese Giant Salamander (*Andrias davidianus*)	8	26	NR	Critically Endangered	Zhu et al. 2014
	Southern Corroboree Frog (*Pseudophryne corroboree*)	11	9	0.146	Critically Endangered	Kosch et al. 2017
	Red-eyed Tree Frog (Agalychnis callidryas)	5	19	0.212	Least Concern	Kiemnec-Tyburczy et al. 2012
	Emerald Glass Frog (*Espadarana prosoblepon*)	5	12	0.145	Least Concern	Kiemnec-Tyburczy et al. 2012
	Masked Tree Frog (*Smilisca phaeota*)	5	11	0.122	Least Concern	Kiemnec-Tyburczy et al. 2012
	Green Frog (*Lithobates clamitans*)	5	16	0.113	Least Concern	Kiemnec-Tyburczy et al. 2012
	Lowland Leopard Frog (*Lithobates yavapaiensis*)	5	9	0.080	Least Concern	Kiemnec-Tyburczy et al. 2012
	Bullfrog (*Lithobates catesbeianus*)	5	12	0.115	Least Concern	Kiemnec-Tyburczy et al. 2012
	Spot-legged Tree Frog (*Polypedates megacephalus*)	11	7	0.115	Least Concern	Zhao et al. 2013
	Omei Tree Frog (*Rhacophorus omeimontis*)	27	20	0.132	Least Concern	Zhao et al. 2013
MHC class IIβ	Reticulated Flatwoods Salamander (*A. bishopi*)	93	5	0.004	Vunerable	This study
	Tiger Salamanader (*A. tigrinum*)	33	9	NR	Least Concern	Bos and DeWoody 2005
	Mountain Steam Salamander (*A. altamirani*)	19	3	0.008	Endangered	Tracy et al. 2015
	Anderson's Salamander (*A. andersoni*)	13	9	0.062	Critically Endangered	Tracy et al. 2015
	Lake Patzcuaro Salamander (*A. dumerilii*)	12	11	0.057	Critically Endangered	Tracy et al. 2015
	Mexican axolotl (*A. mexicanum*)	27	9	NR	Critically Endangered	Tracy et al. 2015 & Richman et al. 2007
	Plateau Tiger Salamander (*A. velasci*)	13	5	0.072	Least Concern	Tracy et al. 2015
	Chinese Giant Salamander (*Andrias davidianus*)	8	17	0.045	Critically Endangered	Zhu et al. 2014
	Wood Frog (*Rana sylvatica*)	334	20	0.060	Least Concern	Savage et al. 2019
	Chiricahua Leopard Frog (*Lithobates chiricahuensis*)	182	5	NR	Vunerable	Savage et al. 2018
	Lowland leopard frog (*Lithobates yavapaiensis*)	128	84	NR	Least Concern	Savage et al. 2016
	Asiatic Toad (*Bufo gargarizans*)	60	8	0.104	Least Concern	Bataille et al. 2015
	Oriental Fire-bellied Toad (*Bombina orientalis*)	20	7	0.049	Least Concern	Bataille et al. 2015
	Whistling Tree Frog (*Litoria verreauxii alpina*)	90	11	0.096	Least Concern	Bataille et al. 2015

We have demonstrated low levels of immune gene diversity, a result that emphasizes the urgency for further conservation and the need to consider genetic diversity as a valuable asset alongside other restoration goals (Bonin et al. 2007). Because the RFS is at an elevated risk from disease, biosecurity should be a priority at all breeding sites. Management should include considerations to preserve and spread unique genetic variants and increase allelic richness across the RFS range. Genetic variation takes thousands of generations to replace, therefore preserving genetic diversity of the reticulated flatwoods salamander will be crucial for conserving this vulnerable species.

Chapter 3. Population structure and migration rates in the reticulated flatwoods salamander (*Ambystoma bishopi*): determining the suitability of human mediated dispersal

Introduction

Amphibian populations have experienced severe declines worldwide, with up to one third of amphibian species currently facing extinction (McCallum 2007, O'Donnell et al. 2017). Drivers of this decline include pollution, climate change, exposure to novel diseases, and habitat loss or fragmentation (McCallum 2007, Grant et al. 2016). Increased habitat fragmentation has inhibited gene flow among amphibian populations, gene flow that may prevent extirpation of populations and extinction of species (Whiteley et al. 2014). Re-establishing or maintaining historical levels of gene flow by reconnecting populations should be a key component of management and a goal of habitat restoration for species with historically connected populations (Dool et al. 2016, Semlitsch et al. 2017). However, modern anthropogenic landscape changes have made it impossible for some species to naturally recolonize extirpated areas of their historic range and human mediated dispersal may be necessary to repatriate species with low vagility.

The reticulated flatwoods salamander (RFS, *Ambystoma bishopi*) is a federally endangered species with a highly fragmented range. Historically, RFS occurred through the southeastern United States in fire maintained longleaf pine (*Pinus palustris*) ecosystems (Palis 1996, Petranka 2010). Over the last several decades this species has declined due to many factors including a change in fire regime from summer fires when breeding habitat is dry to winter fires when habitat is wet so less vegetation is consumed leaving undesirable mid-story vegetation in breeding habitat (Gorman et al. 2013). This species now occurs in only a fraction of its former

range with just six known breeding sites (Farmer et al. 2016, O'Donnell et al. 2017, Semlitsch et al. 2017).

The RFS breeds in ephemeral, fishless ponds dominated by grasses and forbs (Palis 1996, 1997). These ponds are dry during the summer months but fill with rain in the winter. During rain events in October and November, adults migrate to dry pond basins and lay their eggs in anticipation of the seasonal inundation (Palis 1996, 1997). Once the basin fills and the eggs are inundated, the larvae hatch, and eventually metamorphose when the ponds begin to dry in the spring (Palis 1996). This breeding strategy is highly dependent on predictable seasonal rainfall, and if the ponds do not fill or do not stay full all winter, the entire larval cohort can be lost (Chandler et al. 2016, Palis et al. 1996).

Breeding sites consist of several individual ponds that are occupied each year and connected by suitable habitat. Individual salamanders appear to disperse among ponds within a particular breeding site but do not appear to disperse between breeding sites, as estimated from occupancy-based metapopulation models (Brooks et al. 2019). Estimates of dispersal in relation to geographical distance has led the United States Fish and Wildlife Service to define any occupied pond (and a 460-meter radius around it) as a breeding population and any grouping of ponds within 3.2 km of each other (2 miles, USFWS 2015) as a breeding site.

This type of population organization means that genetic structure and migration can be estimated on two scales: a fine, local scale and a large, range-wide scale. Genetic population structure and gene flow have been previously estimated with microsatellite data, and show that there is gene flow and low structure among ponds within the two separate breeding sites on Eglin (Wendt 2017); however, to effectively estimate population structure at small scales, hundreds of genetic markers may be needed because subtle patterns can be obscured when few makers are

used (Rittmeyer and Austin 2014). This is exemplified in tiger salamanders (*Ambystoma tigrinum*) where microsatellite data could not detect patterns of fine-scale structure, but several hundred SNPs could (McCartney-Melstad et al. 2018).

Together with population structure, estimates of contemporary and historic migration rates are important for estimating the connectivity among breeding sites. Historically connected sites with little genetic structure are candidates for human mediated dispersal such as translocations and reintroductions. The International Union for Conservation of Nature (IUCN) defines translocations as the human-mediated movement of living organisms from one area, with release in another. It also defines reintroductions as the intentional movement and release of an organism inside its indigenous range from which it has disappeared (hereafter repatriation, IUCN 2013). Several studies have tested the effectiveness of translocations and repatriations in order to conserve endangered amphibian species. Eastern hellbenders (*Cryptobranchus alleganiensis*), which have declined across their range, have been successfully translocated to several sites in order to supplement existing populations (Kraus et al. 2017, McCallen et al. 2018). Spotted salamanders (*Ambystoma maculatum*) have been repatriated to accelerate restoration by moving egg masses into artificial ponds. These eggs quickly hatched and larval survival was similar to those in the donor ponds (Sacerdote 2009). Overall, mediating species movement has been a successful tool in amphibian conservation and can be used to bolster and expand populations of endangered species.

Genetic tools can be used to accurately measure many natural processes that are difficult to quantify through traditional field techniques. Typical genetic studies require fewer sampling events and are less invasive than field studies, a distinct advantage when species are endangered, occur in low densities, or are elusive (Allendorf et al. 2013, Wang and Shaffer 2017).

Populations can be delineated and barriers to dispersal identified while estimates of migration can be determined without directly observing the movement of tagged animals (Sommer et al. 2013). Sex-biased dispersal can also be measured by comparing different genetic markers such as sex chromosomes or mitochondrial DNA with nuclear genes (Allendorf et al. 2013). Finally, degree of inbreeding can be quantified, even without pedigree data (Allendorf et al. 2013). Genetic tools are powerful methods for determining many important questions relevant to species conservation and management.

Understanding patterns of migration and population structure at the landscape and local scale is necessary to determine the suitability of human mediated dispersal for the RFS. This study estimates genetic structure as well as historic and contemporary migration among extant breeding sites. Assessing connectivity and genetic differentiation among the remaining breeding sites can inform potential repatriations and translocations of RFS in order to begin re-establishing this species across its former range and thus reduce its risk of extinction (Semlitsch et al. 2017).

Methods

Sample Collection

Tissue samples were collected from five RFS breeding sites found on public lands (Figure 2.1). For a full description of collection methods see Chapter 1 (Williams et al. *in prep*). Briefly, samples were collected with dip nets and funnel traps at six ponds on Eglin Air Force base (AFB), Florida between 2011 and 2017. These six ponds included two separate breeding sites, one in the east (n = 4 ponds) and one in the west (n = 2 ponds). In 2018 and 2019

additional RFS samples were collected at five ponds on Escribano Point Wildlife Management Area (WMA), Florida; at one pond at Garcon Point Water Management Area, Florida; and at one pond at Mayhaw WMA, Georgia. Sample sizes at some breeding sites were limited by RFS population size and permission to access sites.

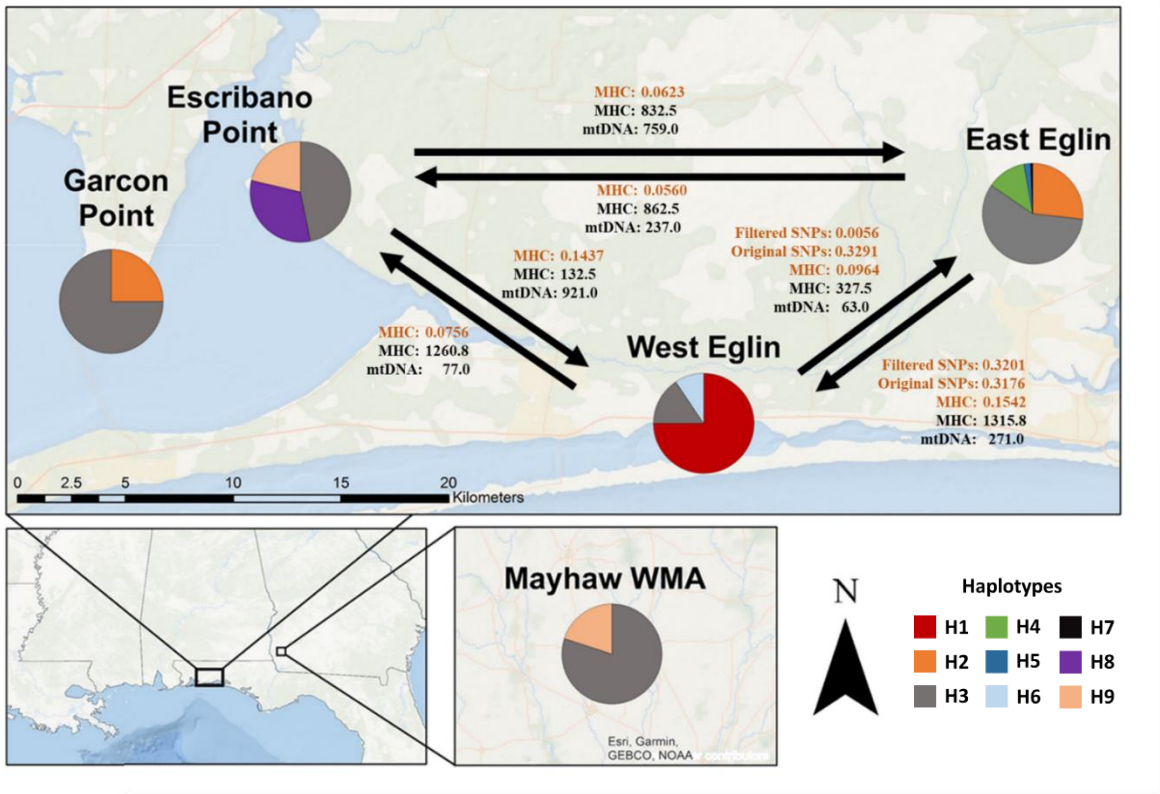

Figure 2.1. Map of sampled RFS breeding sites, arrows indicate migration rates and pie charts display the proportion of haplotypes at each site (size of circle does not reflect sample size). Black wording are estimates of mutation scaled migration rate per generation using Migrate-N while the orange wording are estimates of migration using BayesAss.

Immunome Sequencing

Hundreds of RFS immune genes were sequenced to target single nucleotide polymorphisms (SNPs). To create custom RNA baits, the axolotl (*Ambystoma mexicanum*) transcriptome (Bryant et al. 2017) was filtered by the gene ontology term ‘immune response’

using the GO2TR 1.0.8 pipeline (Gene Ontology to Target Region, Elbers & Taylor 2015), which retained all exons related to the immune system (hereafter, immunome; Ortutay & Vihinen 2006). Using these exons, Arbor Biosciences (Ann Arbor, Michigan, USA) designed custom MYBaits 120-bp biotinylated RNA baits with 2x tiling to capture the immunome of the RFS (hereafter, baits).

In 2017, 96 samples from Eglin AFB (east = 73, west = 23) were selected for the target enrichment experiment. Samples from other sites were not included because non-Eglin samples were not available until after immunome sequencing was completed in 2018. Libraries were prepared using 10ng of starting DNA and a KAPA HyperPlus Illumina prep kit in combination with dual-indexed Illumina adapters (KAPA Biosystems, Indianapolis, IN, USA) to create sixteen equimolar pools containing six libraries each (i.e., 96 libraries in 16 pools). These pooled libraries then underwent sequence capture following the MyBaits sequence capture protocol version 3.0, by combining libraries with baits and incubating in solution for 21 hours at 65°C. Then pools were washed to retain only "captured" baits and amplified with 14 PCR cycles. Finally, libraries were cleaned using KAPA pure beads (Indianapolis, IN, USA). To achieve adequate coverage, all 96 captured libraries were sequenced twice on mid-output flow cells of an Illumina NextSeq system at Pennington Biomedical Research Center (Baton Rouge, LA) using 75-bp paired end reads.

Raw sequence reads were demultiplexed using the Illumina BaseSpace platform permitting zero mismatches in the dual-indexed 8-bp barcodes. Adapter quality trimming was performed on demultiplexed paired end reads using BBDuk 38.16 (https://sourceforge.net/projects/bbmap/), and the following options: ktrim=r, k=23, mink=11, hdist=1, tpe, tbo, qtrim=rl, trimq=15, with Illumina TruSeq adapters as the reference. Next,

quality and adapter trimmed paired-end reads were mapped to the axolotl 3.0.0 reference genome (https://axolotl-omics.org/dl/AmexG_v3.0.0.fa.gz) using BBMap 38.16 (https://sourceforge.net/projects/bbmap/) and the vslow and usejni options. SAM files were converted to BAM files with SAMtools 1.9 (Li et al. 2009). Picard 2.18.10 (http://broadinstitute.github.io/picard) was used to clean, sort, add read groups, and mark duplicates. The program CallVariants 38.16 (https://sourceforge.net/projects/bbmap/) was used to call variants by ignoring duplicates and keeping variants with quality scores greater than or equal to 27. Finally, only di-allelic SNPs with a quality score greater than or equal to 27, and genotype missingness of 5 % or less, were retained using VCFtools 0.1.15 (Danecek et al. 2011).

SNPs were tested by pond for linkage disequilibrium and Hardy-Weinberg equilibrium (HWE) using VCFtools, geno-chisq and hardy tests. The p.adjust function in R (Team 2018) was then used to correct for multiple tests using the false discovery rate (FDR, Benjamini & Hochberg 1995). Originally, SNPs that had a FDR less than 0.05 in at least 5 ponds were discarded. For this original dataset H_O was 42% while H_E was between 26 – 28% (Table 2.1). Gene duplication in the RFS, a pattern observed in other amphibians (McCartney-Melstad et al. 2018; Waples et al. 2015), can lead to heterozygote excess causing $H_O >> H_E$. This possible gene duplication prompted re-filtering of the SNP data using more stringent conditions. For the filtered dataset, SNPs that had a FDR less than 0.05 in one or more ponds were discarded. Finally, BayeScan 2.1 (Foll and Gaggiotti 2008) was used to predict if SNPs were under selection. Neutral SNPs were used to estimate population structure and gene flow under neutral expectations. SNPs under selection were of interest to better understand disease resilience and immune gene diversity since pathogens contribute substantially to the world-wide amphibian

decline (Carey and Alexander 2003, McCallum 2007, Grant et al. 2016, O'Donnell et al. 2017); however, no SNPs were identified as being under selection in either dataset.

Table 2.1. Allelic richness (AR), observed heterozygosity (H_O), expected heterozygosity (H_E), and inbreeding coefficient (F_{IS}) for the original dataset and filtered dataset (parentheses).

Site	*n*	AR	H_O	H_E	F_{IS}
Pond 004	24	1.63 (1.36)	0.45 (0.13)	0.27 (0.11)	-0.61 (-0.22)
Pond 005	24	1.65 (1.41)	0.46 (0.16)	0.28 (0.14)	-0.63 (-0.22)
Pond 053	19	1.63 (1.37)	0.46 (0.14)	0.27 (0.12)	-0.64 (-0.24)
Pond 212	6	1.64 (1.40)	0.49 (0.17)	0.28 (0.14)	-0.71 (-0.29)
Pond 015	19	1.66 (1.43)	0.46 (0.17)	0.28 (0.14)	-0.62 (-0.23)
Pond 032	4	1.75 (1.66)	0.41 (0.19)	0.27 (0.16)	-0.47 (-0.22)
East Eglin	73	1.82 (1.38)	0.41 (0.15)	0.26 (0.12)	-0.58 (-0.18)
West Eglin	23	1.95 (1.44)	0.42 (0.18)	0.27 (0.15)	-0.63 (-0.17)

PGDSpider 2.1.1.5 (Lischer & Excoffier 2012) was used to convert SNPs in VCF format to inputs suitable for population genetic programs. All analyses were conducted for both datasets. Allelic richness (AR), observed (H_O) and expected heterozygosity (H_E), pairwise F_{ST} (Weir and Cockerham 1984), and principle component analysis (PCA) were estimated in hierfstat version 0.04-22 (Goudet 2005). The inbreeding coefficient for each breeding site (F_{IS}, Weir and Cockerham 1984) was estimated in GenePop v4.6 (Raymond and Rousset 1995, Rousset 2008). Recent patterns of migration were estimated with BayesAss 3.0 (Wilson and Rannala 2003). BayesAss estimates migration rate over the last three generations by calculating the probability of migrant ancestry for all individuals, assigning them as either a non-migrant, 1st generation, or 2nd generation migrants. Multiple iterations of the analysis were run using different seeds to ensure convergence of models. For all runs, a burn-in of $2x10^6$ followed by

$1x10^6$ sampling iterations with a sampling interval of 100 were used. Finally, fastSTRUCTURE 1.0 (Raj et al. 2014) and Admixture 1.3.1 (Alexander et al. 2009) were run to assess population admixture using ancestry models from K=1 to K=7 to infer the number of populations (K) from the data.

MHC and mtDNA Sequencing

To include other breeding sites and multiple marker types in the analyses, regions of the major histocompatibility complex (MHC) and mitochondria were sequenced. A full explanation of DNA extraction, PCR, and Sanger sequencing methods can be found in Chapter 1 (Williams et al. *in prep*). Briefly, across all breeding sites, both MHC class Iα exon 3 and class IIβ exon 2 were sequenced for 84 individuals while the mitochondrial control region (D-loop) was sequenced for 226 individuals (Table 2.2, Pauley et al. 2007). Poor amplification and sample availability ultimately reduced MHC sample size. An analysis of molecular variance (AMOVA) was conducted for MHC and mtDNA using Arlequin 3.5 (Excoffier et al. 2005). Samples from Mayhaw and Garcon were removed from further analysis because of low sample sizes, but for Eglin East, Eglin West, and Escribano, pairwise F_{ST} (Weir and Cockerham 1984) was calculated in hierfstat version 0.04-22 using both MHC loci coded as alleles (each distinct sequence was given a number e.g. allele 01). Φ_{ST} was calculated in Arlequin 3.5 using mitochondrial haplotype frequencies. PCAs and program STRUCTURE v2.3.4 (Pritchard et al. 2000) were run for MHC genes as described for SNP data, and the inbreeding coefficient was estimated in GenePop v4.6. PCAs and STRUCTURE were not calculated for mitochondrial DNA because both programs require diploid data. Recent migration rates were estimated for MHC and mitochondria haplotypes at Eglin East, Eglin West, and Esribano with program BayesAss 3.0 and the

conditions described above. Historic migration rates (>5 generations) were estimated by Bayesian inference in Migrate v3.7.2 (hereafter Migrate-N, Beerli and Felsenstein 1999, 2001). This program estimates two metrics, the mutation scaled population size (Θ), which is calculated as $\Theta = 4N_e\mu$ where N_e is effective population size and μ is mutation rate, and it calculates a mutation scaled migration rate measured as the number of migrants per generation calculated as m/μ where m is the migration rate and μ is the mutation rate. Here a full migration matrix model was used, which assumes direct gene flow between all populations. After testing multiple parameters, three long chains with a burn-in of $5x10^6$ were run and, to avoid autocorrelation, samples were taken every 50 steps for $5x10^4$ iterations. For mitochondrial DNA, a mitochondrial haplotype network was created using a minimum joining network in Popart 1.7 (Figure 2.2, Bandelt et al. 1999).

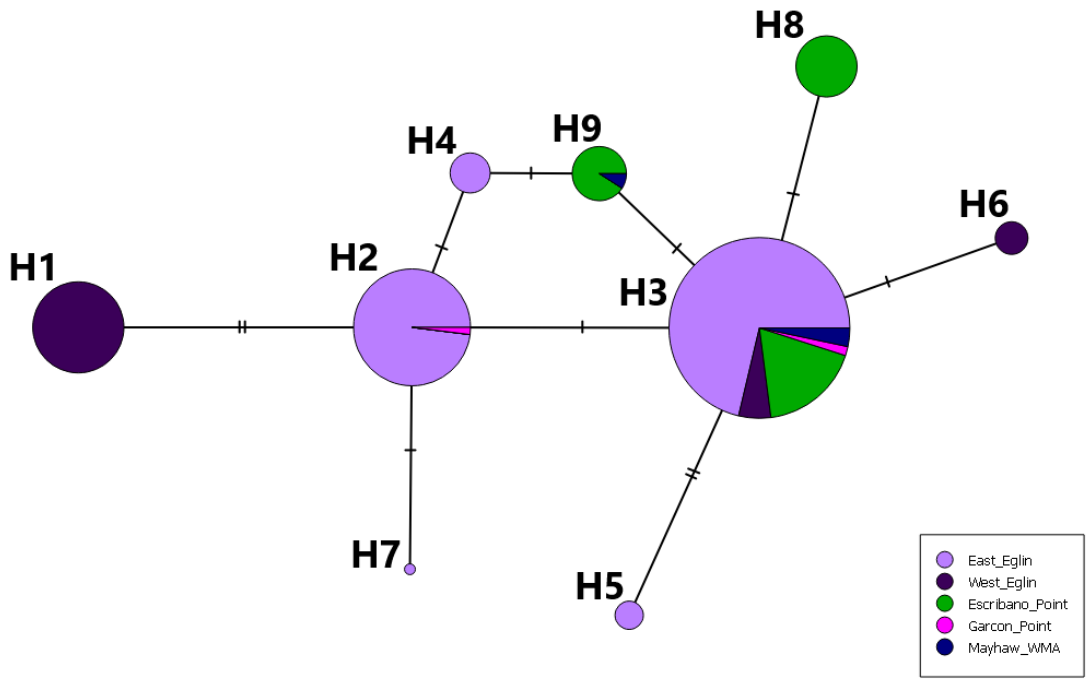

Figure 2.2. Haplotype network of mitochondrial D-loop sequences. Circle size is proportional to the number of individuals per haplotype and each dash represents a single nucleotide polymorphism.

Table 2.2. Sample sizes for each genetic marker by breeding site. Numbers given for MHC are the numbers of individuals sequenced at both MHC class Iα and IIβ.

Site	MHC	mtDNA	SNP
Eglin East	29	143	73
Pond 004	6	51	24
Pond 005	8	54	24
Pond 053	10	24	19
Pond 212	5	14	6
Eglin West	18	30	23
Pond 015	12	24	19
Pond 032	6	6	4
Escribano	28	46	0
Borrow	5	10	0
Cluster	3	11	0
Honey	5	7	0
Ghost	6	9	0
Tropedo	7	8	0
Garcon	4	3	0
Mayhaw	5	5	0
Total	84	227	96

Results

Immunome Sequencing

After quality control filtering, 263,127,494 reads were assignable with 2,740,911 ± 2,328,524 (mean ± SD) reads assigned per individual (range = 477,444 – 14,876,290). Ultimately, 95% of unique reads were successfully aligned after 9% of the original reads were removed as PCR or optical duplicates. After alignment to the axolotl genome, 183 SNPs were

identified. For the original dataset, 166 SNPs were polymorphic, in HWE and in linkage equilibrium but for the filtered dataset 90 SNPs were polymorphic, in HWE and in linkage equilibrium.

Genetic Variation

In the original SNP dataset, allelic richness was 1.82 in East Eglin and 1.95 in West Eglin. H_O at both sites was between 41 – 42% while H_E was between 26 – 28% (Table 2.1). The inbreeding coefficient at East Eglin was -0.58 and -0.63 in West Eglin (Table 2.1). For the filtered dataset, allelic richness was 1.38 in East Eglin and 1.44 in West Eglin (Table 2.1). At East Eglin and West Eglin, H_O was 15% and 18% respectively, while H_E was 12% at East Eglin and 15% at West Eglin (Table 2.1).

Low genetic variation was observed at both MHC exons. For class Iα only three alleles were found with a nucleotide diversity of 0.0013, H_E of 19.9%, and a H_O of 16.8%. MHC class IIβ had five alleles with a nucleotide diversity of 0.0044, H_E of 53.7%, and H_O of 34.4% (Chapter 1, Williams et al. *in prep*). At East Eglin, West Eglin, and Escribano, F_{IS} for MHC class IIβ was 0.304, 0.339, and 0.479 respectively. Contrastingly, F_{IS} for MHC class Iα was lower at these three sites with values of 0.106, -0.120, and 0.084. Nine mitochondrial haplotypes were observed, two of which had already been described in Pauley et al. (2007; Genbank accession numbers H2: EU517607.1 and H3: EU517606.1) while the other seven were previously undescribed. Of the nine haplotypes, one occurred at all breeding sites (H3) while two others (H2, H9) were found at multiple breeding sites (Figure 2.1, Chapter 1, Williams et al. *in prep*).

Population Structure

Pairwise F_{ST} was estimated with immunome SNP data on Eglin and MHC data on Eglin and Escribano. Using the original SNP dataset for individual ponds within breeding sites on Eglin, pairwise F_{ST} was ≤ 0.012 while F_{ST} between Eastern and Western Eglin was 0.002 (Table 2.3). With the filtered dataset, F_{ST} between ponds within breeding sites was ≤ 0.056 and between Eastern and Western Eglin was 0.004 (Table 2.3). For MHC loci, F_{ST} values between breeding sites ranged from -0.0067 to 0.0913 (Table 2.4). Values for MHC between ponds within breeding sites could not be calculated due to small sample sizes at individual ponds.

Table 2.3. F_{ST} calculated with SNP data by pond on Eglin. F_{ST} below the diagonal where values from the original dataset are on top and values from the filtered dataset are on bottom in parenthesis. Euclidean distance (km) is given above the diagonal. Bolded values are significant $p < 0.05$. Pairwise F_{ST} between the two breeding sites for the original dataset was 0.002, and 0.004 for the filtered dataset.

	Pond 004 [East]	Pond 005 [East]	Pond 053 [East]	Pond 212 [East]	Pond 015 [West]	Pond 032 [West]
Pond 004 [East]	-	0.46	0.28	0.48	13.67	13.54
Pond 005 [East]	0.0012 (0.0074)	-	0.36	0.94	13.45	13.32
Pond 053 [East]	-0.0001 (0.0021)	0.0022 (0.0116)	-	0.68	13.4	13.26
Pond 212 [East]	0.0010 (0.0047)	-0.0002 (0.0073)	0.0022 (0.0131)	-	13.9	13.77
Pond 015 [West]	0.0005 (0.0057)	-0.0002 (0.0002)	0.0026 (0.0062)	0.0016 (0.0012)	-	0.14
Pond 032 [West]	0.0199 (**0.0423**)	0.0130 (0.0208)	0.0257 (**0.0558**)	0.0246 (**0.0312**)	0.0120 (0.0176)	-

Table 2.4. F_{ST} calculated with MHC data by breeding site. F_{ST} below the diagonal and Euclidean distance (km) above the diagonal. Bolded values are significant $p < 0.05$.

	Eglin East	Eglin West	Escribano
Eglin East	-	13.01	30.17
Eglin West	-0.007	-	19.64
Escribano	**0.091**	**0.082**	-

The mitochondrial control region was used to estimate Φ_{ST} between individual ponds within Eglin or Escribano and between the three breeding sites. For ponds within East Eglin, Φ_{ST} values ranged from -0.1686 to 0.2023 while the pairwise comparison within the two West Eglin ponds was 0.0571 (Table 2.5). On Escribano, Φ_{ST} values were between -0.0631 and 0.4204 (Table 2.6). When individual ponds within breeding sites were examined more closely, the highest Φ_{ST} values (0.28 – 0.87) were between ponds separated by more than 1.5 km. Ponds less than 1.5 km apart had Φ values below 0.203. Between the breeding sites of East Eglin, West Eglin, and Escribano, Φ_{ST} ranged from 0.1518 to 0.3559 (Table 2.7). Haplotypes overlapped broadly across all RFS breeding sites and ponds within sites (Figure 2.1 and 2).

Table 2.5. Φ_{ST} calculated with mtDNA data by pond on Eglin. Φ_{ST} below the diagonal and Euclidean distance (km) above the diagonal. Bolded values are significant $p < 0.05$.

	Pond 004 [East]	Pond 005 [East]	Pond 053 [East]	Pond 212 [East]	Pond 015 [West]	Pond 032 [West]
Pond 004 [East]	-	0.46	0.28	0.48	13.67	13.54
Pond 005 [East]	0.033	-	0.36	0.94	13.45	13.32
Pond 053 [East]	-0.018	**0.065**	-	0.68	13.40	13.26
Pond 212 [East]	0.068	**0.202**	0.025	-	13.90	13.77
Pond 015 [West]	**0.396**	**0.401**	**0.427**	**0.559**	-	0.14
Pond 032 [West]	**0.549**	**0.541**	**0.608**	**0.874**	0.057	-

Table 2.6. Φ_{ST} calculated with mtDNA data by pond on Escribano. Φ_{ST} below the diagonal and Euclidean distance (km) above the diagonal. Bolded values are significant $p < 0.05$.

	Borrow	Cluster	Honey	Ghost	Torpedo
Borrow	-	1.01	3.40	3.30	2.80
Cluster	-0.063	-	2.34	2.28	2.33
Honey	**0.354**	**0.400**	-	0.13	0.53
Ghost	0.287	**0.361**	-0.087	-	0.63
Torpedo	**0.386**	**0.420**	-0.147	-0.030	-

Table 2.7. Φ_{ST} calculated with mtDNA data by breeding site. Φ_{ST} below the diagonal and Euclidean distance (km) above the diagonal. Bolded values are significant $p < 0.05$.

	Eglin East	Eglin West	Escribano
Eglin East	-	13.01	30.17
Eglin West	**0.3559**	-	19.64
Escribano	**0.1518**	**0.3536**	-

AMOVA results with MHC data indicated little population structure: only 9.53% of the total variation was among populations (Table 2.8). Greater population structure was detected with mitochondrial data: 25.49% of the total variation was among populations (Table 2.8).

Table 2.8. AMOVA as estimated with MHC and mtDNA data.

Markers	Source of Variation	Degrees of Freedom	Sum of Squares	Percentage Variation
MHC Iα & IIβ	Among Breeding Sites	4	8.42	9.53
	Among Individuals Within Breeding Sites	85	46.86	19.53
	Within Individuals	90	32	70.95
mtDNA	Among Breeding Sites	4	14.56	25.49
	Within Individuals	233	67.97	74.51

Programs fastSTRUCUTRE and STRUCTURE cannot calculate ΔK when K = 1 so to investigate K = 1 – 7 for this data set we used distruct plots as well as maximized marginal

likelihood for fastSTRUCTURE and log likelihood for STRUCTURE. With both SNP datasets, fastSTRUCTURE suggested a single population (K = 1) on Eglin according to the model that maximized marginal likelihood, this result was confirmed by comparing distruct plots of K = 1 – 3 (Figure 2.3). Program Admixture also suggested a single population on Eglin based on the cross-validation (CV) values for K = 1 – 7 in both datasets (Table 2.9). For MHC data at Eglin and Escribano, program STRUCTURE suggested two populations using ΔK, but one population using log likelihood values. To further evaluate K=2, distruct plots were compared (Figure 2.3). K = 2 shows no distinct patterns between populations and so K=1 was accepted. These results are supported by the PCAs obtained for both SNP and MHC data (Figures 2.4 – 6). SNP data clustered in a single group regardless of collection location or dataset (Figure 2.4 and 5), similarly, MHC data showed no discernable pattern based on sampling site (Figure 2.6).

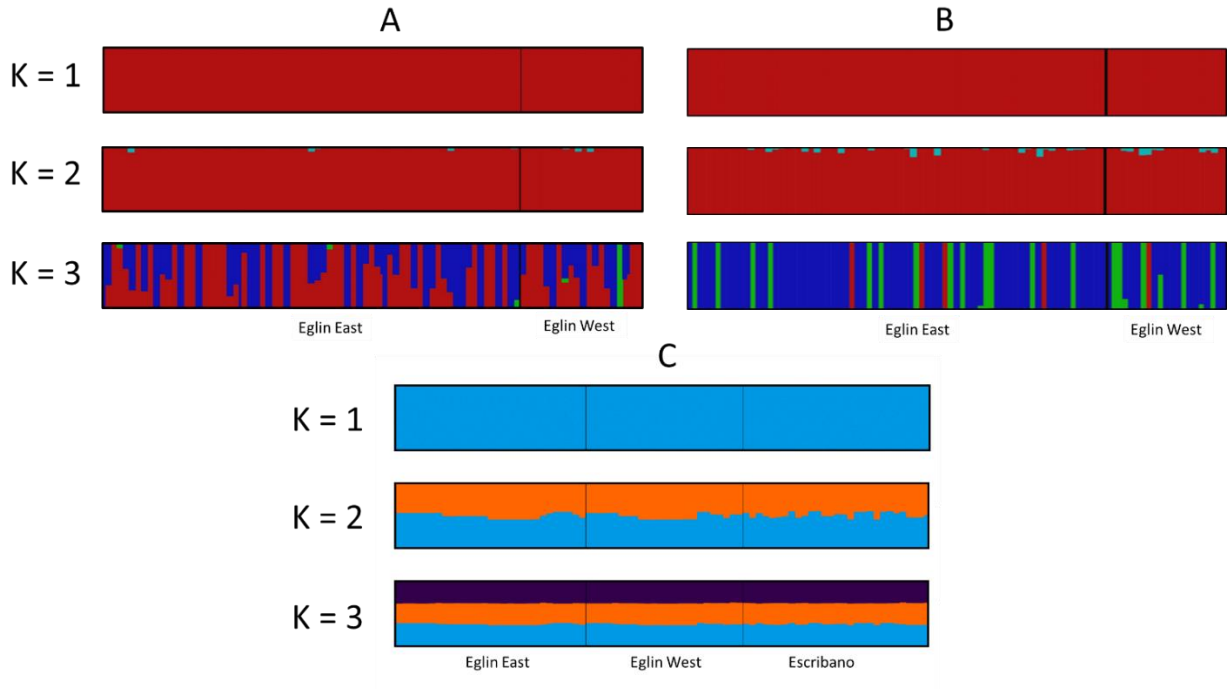

Figure 2.3. Distruct plots for original SNP dataset (A), filtered SNP dataset (B), and for MHC class Iα and IIβ (C).

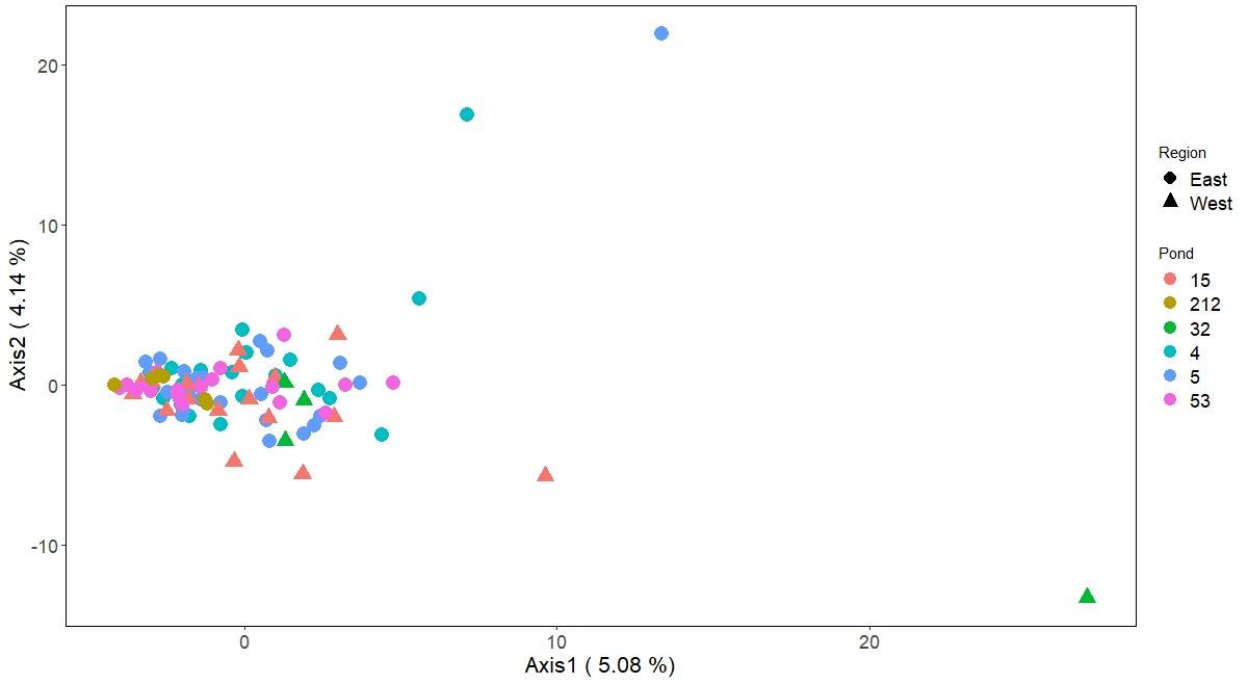

Figure 2.4. PCA analyses of immunome SNP markers for Eglin AFB using the original dataset.

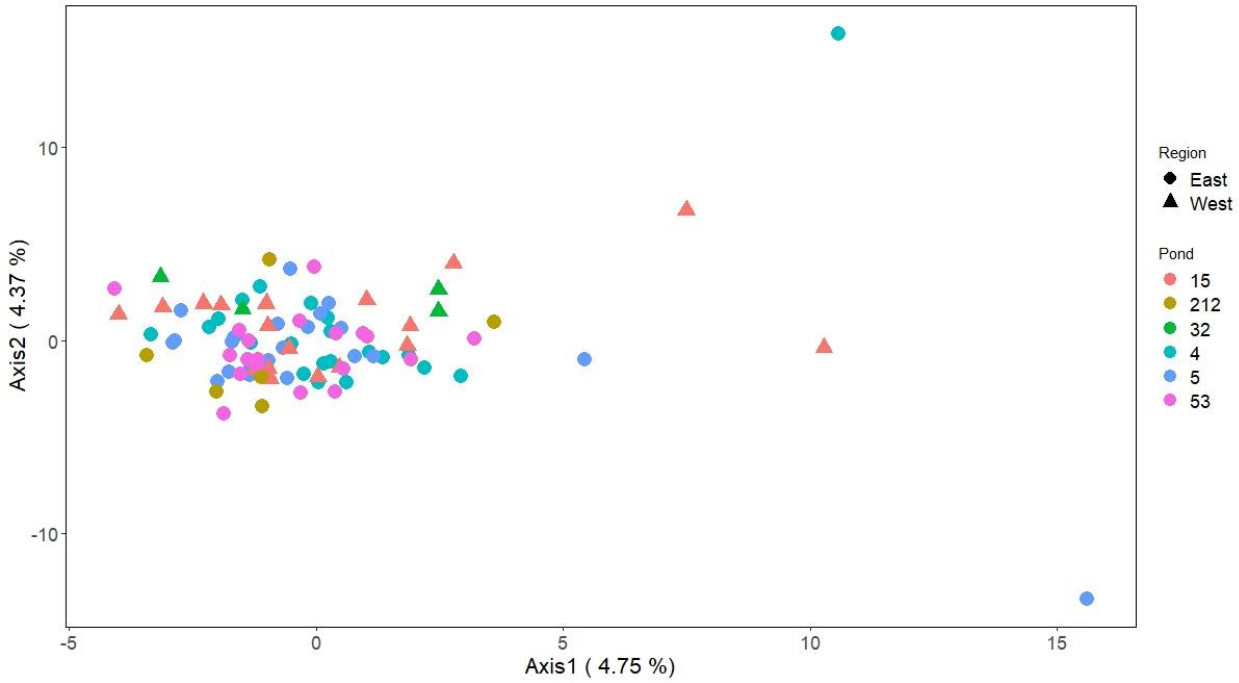

Figure 2.5. PCA analyses of immunome SNP markers for Eglin AFB using the filtered dataset.

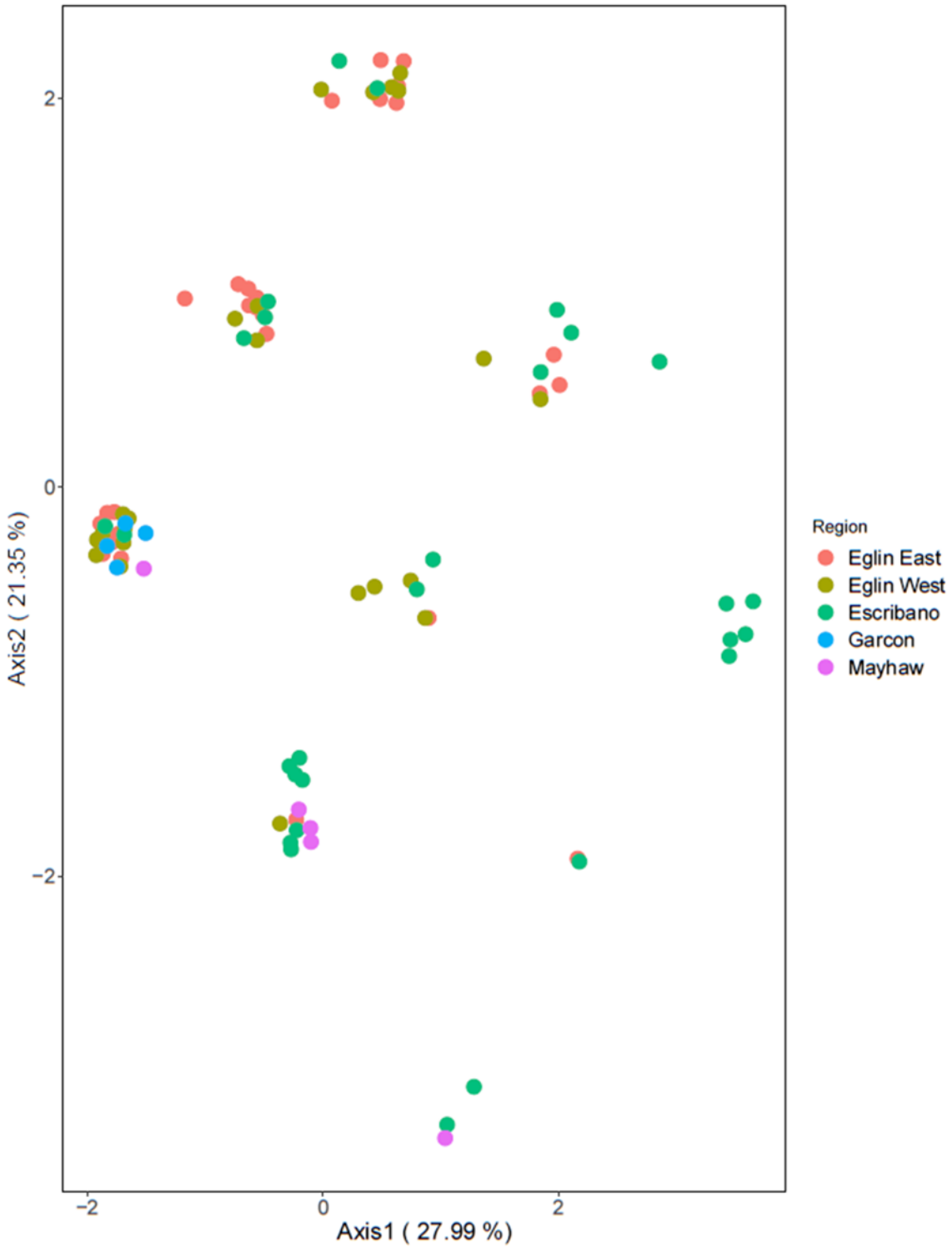

Figure 2.6. PCA analyses of MHC class I & II for all breeding sites.

Table 2.9. Cross validation (CV) values for Admixture for K=1 – 7 using both SNP datasets.

Populations	Original Dataset (CV)	Filtered Dataset (CV)
K = 1	0.22664	0.27783
K = 2	0.24503	0.31485
K = 3	0.25848	0.35503
K = 4	0.26879	0.38147
K = 5	0.28971	0.40472
K = 6	0.29487	0.41595
K = 7	0.29913	0.42432

Gene Flow

For program Migrate-N, the mode migration estimate for MHC and mitochondrial data was reported, because for MHC markers, the mean, median, and mode were almost identical (Table 2.10), but for mitochondrial estimates, the mode better represented the peak of the distribution on the curve (Figures 2.7 and 8). For mitochondrial data, migration rates were not multiplied by four (to account for mtDNA N_E) to equate them with migration rates for a nuclear marker, instead they were left unadjusted to estimate migration for this haploid, maternally inherited marker. Migrate-N estimates using MHC and mitochondrial data had wide posterior distributions for both migration and Θ estimates, and thus only general patterns of migration are discussed. Migration rates for MHC class IIβ were highest from East to West Eglin. Migration rates were also high for West Eglin to Escribano, but low for Escribano to West Eglin and West Eglin to East Eglin. Migration rates between East Eglin and Escribano were moderate and almost equal both directions (Table 2.10, Figure 2.7). For mitochondrial data, models gave wide estimates with long tails. Estimates of migration with mitochondrial data were highest from Escribano to East and West Eglin while migration out of West Eglin was the lowest (Table 2.10, Figure 2.8). Although the lowest confidence intervals for many mitochondrial migration rates were at or near zero, mean, median, and mode estimates were always more than 60 individuals.

MHC class Iα estimates were uninformative, probably because range-wide genetic variation was very low.

Table 2.10. Migrate-N posterior distribution table of theta (Θ) and migration rates using SNPs, MHC class IIβ, and mtDNA.

Marker	Parameter	2.50%	25.0%	Mode	75.0%	97.5%	Median	Mean
MHC IIβ	$\Theta_{East\ Eglin}$	0.0064	0.0089	0.0108	0.0148	0.0253	0.0134	0.0144
MHC IIβ	$\Theta_{West\ Eglin}$	0.0042	0.0056	0.0090	0.0138	0.0272	0.0127	0.0141
MHC IIβ	$\Theta_{Escribano}$	0.0049	0.0065	0.0108	0.0169	0.0294	0.0154	0.0160
MHC IIβ	East Eglin -> West Eglin	1111.7	1241.7	1315.8	1388.3	1533.3	1320.8	1321.3
MHC IIβ	East Eglin -> Escribano	678.3	795.0	862.5	933.3	1078.3	872.5	874.5
MHC IIβ	West Eglin -> East Eglin	280.0	338.3	372.5	406.7	471.7	375.8	375.6
MHC IIβ	West Eglin -> Escribano	1030.0	1176.7	1260.8	1345.0	1511.7	1267.5	1269.7
MHC IIβ	Escribano -> East Eglin	701.7	785.0	832.5	880.0	973.3	837.5	837.4
MHC IIβ	Escribano -> Wet Eglin	60.0	105.0	132.5	160.0	213.3	137.5	136.8
mtDNA	$\Theta_{East\ Eglin}$	0.0004	0.0007	0.0010	0.0013	0.0020	0.0011	0.0012
mtDNA	$\Theta_{West\ Eglin}$	0.0001	0.0002	0.0003	0.0005	0.0009	0.0004	0.0004
mtDNA	$\Theta_{Escribano}$	0.0001	0.0003	0.0005	0.0007	0.0012	0.0006	0.0006
mtDNA	East Eglin -> West Eglin	0.0	10.0	271.0	1008.0	2624.0	997.0	1135.9
mtDNA	East Eglin -> Escribano	0.0	0.0	237.0	998.0	2646.0	999.0	1140.3
mtDNA	West Eglin -> East Eglin	0.0	0.0	63.0	396.0	1614.0	397.0	549.3
mtDNA	West Eglin -> Escribano	0.0	0.0	77.0	714.0	2422.0	715.0	908.3
mtDNA	Escribano -> East Eglin	4.0	326.0	759.0	1394.0	2630.0	1167.0	1258.0
mtDNA	Escribano -> West Eglin	84.0	524.0	921.0	1734.0	2824.0	1355.0	1411.2

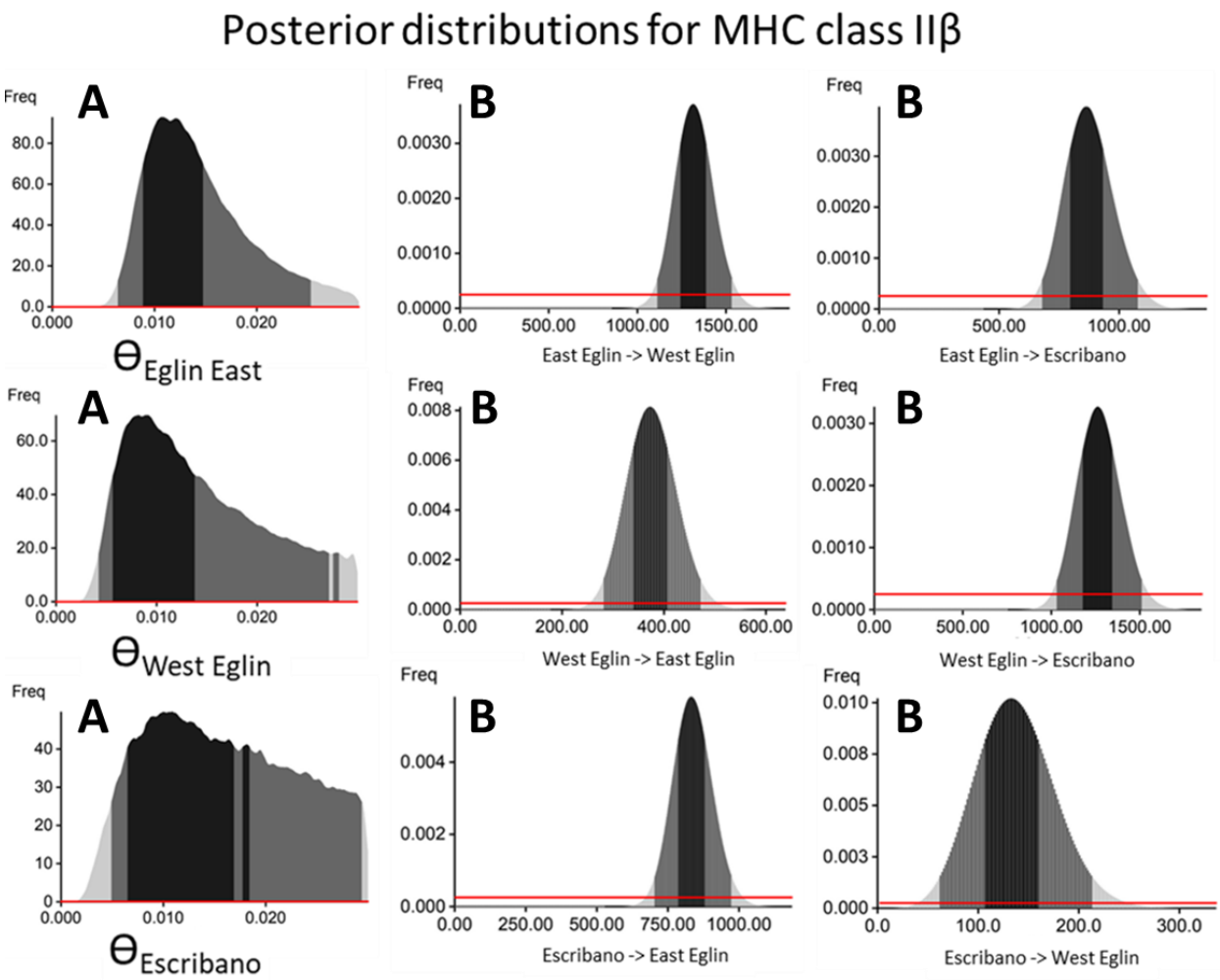

Figure 2.7. Migrate-N posterior distribution of theta (Θ) A, and mutation scaled migration rate per generation B using MHC class IIβ. The red lines are prior distributions used in the model.

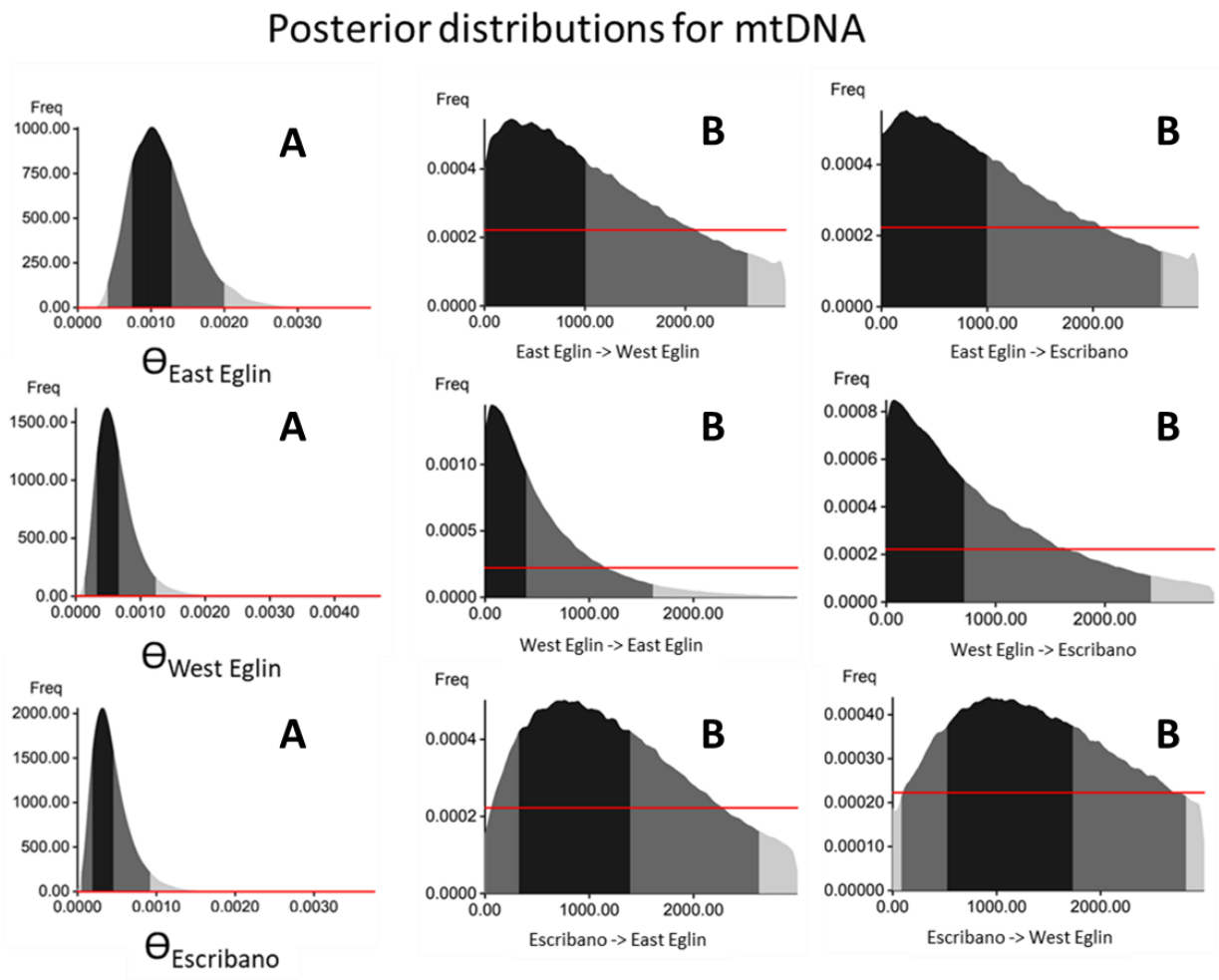

Figure 2.8. Migrate-N posterior distribution of theta (Θ) A, and mutation scaled migration rate per generation B using mitochondrial DNA. The red lines are prior distributions used in the model.

Finally, migration rates as estimated with SNP data in BayesAss showed two patterns. For the original dataset, estimates were fairly symmetrical: 31.8% of individuals in the West were migrants from the East while 32.9% of individuals in the East were migrants from the West (Table 2.11). For the filtered dataset estimates were asymmetrical: 32.0% of individuals in the West were migrants from the East while 0.6% of individuals in the East were migrants from the West (Table 2.11). BayesAss estimates for MHC data were generally lower than estimates

obtained with SNP data. West Eglin had the most individuals of migrant ancestry (14.4 - 15.4%) while East Eglin and Escribano had fewer migrants (5.6 to 8.8%; Table 2.11).

Table 2.11. BayesAss immigration rate estimates with 95% credible interval using MHC and both SNP datasets.

Marker	Source	Destination	Migration Rate	95% credible interval
MHC	Eglin East	Eglin West	0.1542	0.0818 - 0.2266
MHC	Eglin East	Escribano	0.0560	0.0172 - 0.0948
MHC	Eglin West	Eglin East	0.0964	0.0398 - 0.1362
MHC	Eglin West	Escribano	0.0756	0.0298 - 0.1214
MHC	Escribano	Eglin East	0.0623	0.0240 - 0.1006
MHC	Escribano	Eglin West	0.1437	0.0743 - 0.2131
Original SNP	East Eglin	West Eglin	0.3176	0.3025 - 0.3327
Original SNP	West Eglin	East Eglin	0.3291	0.3249 - 0.3333
Filtered SNP	East Eglin	West Eglin	0.3201	0.3072 - 0.3330
Filtered SNP	West Eglin	East Eglin	0.0056	0.0000 - 0.0114

Discussion

SNP data showed little population structure and high levels of gene flow among RFS ponds on Eglin, a result that is consistent for both datasets and all analyses (F_{ST}, PCA, fastStructure, and Admixture). Since there was little genetic structure and high gene flow among ponds, data from ponds within each breeding site were combined to examine population structure and gene flow between breeding sites for all genetic markers (SNP, MHC, mtDNA). At this larger scale, SNP data continued to support a lack of genetic structure and high levels of gene flow between the two Eglin breeding sites, a result supported again by all analyses (F_{ST}, AMOVA, PCA, fastStructure, Admixture, and BayesAss). Data from all marker types suggest migration between the three largest breeding sites (East Eglin, West Eglin, and Escribano). Both

Migrate-N and BayesAss suggest that West Eglin receives more immigrants from and contributes fewer emigrants to Escribano and East Eglin overall (BayesAss: SNP and MHC, Migrate-N: mtDNA). Asymmetrical gene flow is most pronounced on Eglin with an approximate 3:1 migration rate between East and West Eglin (Migrate-N) as estimated with MHC and mitochondrial markers. This asymmetrical migration rate may be caused by directional water flow, particularly flow during heavy rain events, which commonly occur in the breeding season. Heavy rain may create water flow that facilitates migration in a westward direction but limits eastward migration. This hypothesis needs to be explored further by examining water flow and digital elevation models. Asymmetrical migration rates could also be an artifact of different demographic history between sites. Particularly, differences in population sizes may impact the number of migrants leaving a site or a more severe bottleneck at one site could remove genetic variants that are found at other sites, this would create an uneven pattern of diversity which the program interprets as asymmetrical migration.

Other studies have found more population structure in fall breeding ambystomatids, such as RFS, than in spring breeders on the same landscape. Ringed salamanders (*Ambystoma annulatum*) and marbled salamanders (*Ambystoma opacum*), both fall breeders, showed more population structure on Fort Leonard Wood, MO than spotted salamanders, which breed in the spring (Peterman et al. 2015, Burkhart et al. 2016). Estimated genetic dispersal distance for ringed and spotted salamanders was 1700m and 2050m respectively, indicating that both species can disperse but factors beyond dispersal contribute to the difference in genetic structure (Peterman et al. 2015). Selecting suitable egg laying habitat is more difficult in the fall because ponds have not yet filled with water, as compared to spring conditions when water is already present. Consequently, adults must anticipate habitat that will be inundated, perhaps increasing

selective pressure to choose breeding sites based on cues such as previous experience or pond-associated vegetation (Brooks et al. 2019). This pressure to select breeding sites using previous experiences and vegetation may contribute to greater philopatry in fall breeding salamanders thus increasing genetic structure (Peterman et al. 2015, Burkhart et al. 2016).

Another RFS study, using microsatellite markers at the same ponds on Eglin, reported microsatellite average F_{ST} values within East Eglin as 0.042 (0.009 – 0.086) and within the two sampled ponds in West Eglin as 0.025, while comparisons of ponds between East and West Eglin averaged 0.106 (0.079 – 0.135). BayesAss estimates with microsatellite data showed low immigration rates between ponds averaging 0.020 (0.002 – 0.273; Wendt 2017). Although estimates obtained with microsatellite, SNP and MHC markers cannot be compared directly, an examination of overall patterns is useful. F_{ST} estimates between Eglin ponds are low for both microsatellite and SNP data, but microsatellite data are estimating higher F_{ST} values between breeding sites than SNP and MHC data.

In contrast to nuclear markers, mitochondrial structure was high between all breeding sites and even indicated some structure within breeding sites (i.e. between ponds on breeding sites: Table 2.6 and 7). The disparity in genetic structure and dispersal estimates for nuclear and mitochondrial DNA is indicative of male-biased dispersal, a pattern observed in other amphibians including the red-backed salamander (*Plethodon cinereus*) and the alpine salamander (*Salamandra atra*, Liebgold et al. 2011, Helfer et al. 2012). Females may be capable of moving long distances, but as fall breeders that rely on cues like previous experience to select suitable egg laying habitat, they may have a stronger philopatric connection to their natal pond in contrast to males which orient based on receptive females, and thus females do not disperse as widely (Peterman et al. 2015, Burkhart et al. 2016, Moore and Whiteman 2016).

Although there was little mitochondrial structure over short distances, analyses indicated that Φ_{ST} increased considerably when ponds were separated by more than 1.5km, a value similar to the dispersal distances suggested in Brooks et al. (2019). Notably, although Escribano is treated as one breeding site by the USFWS, mitochondrial data showed that highly philopatric females may effectively occupy two distinct breeding sites at this location: Borrow and Cluster ponds, which are separated by approximately 2.3 kilometers from the second group, Honey, Torpedo, and Ghost. However, it is difficult to estimate the precise relationship between dispersal and distance because distances between ponds have a clumped distribution (currently occupied ponds are either 0.1 – 1.0 km apart, 2.5 – 3.5km apart, or >10.0 km apart) and do not fall on a continuum. Mitochondrial data suggests that females typically do not disperse more than 1.5km but that estimate may be low because there were no sampled ponds in the 1.0 – 2.5km range.

Managing all RFS populations in a metapopulation context, in which there is limited gene flow among breeding sites, is an option that may maintain genetic diversity over the long-term. In theory, as different alleles drift to fixation in individual breeding sites, global heterozygosity is effectively frozen in the total population, but there is still sufficient gene flow to prevent inbreeding over the long term within breeding sites and spread advantageous alleles across the species' range (Allendorf et al. 2013). In practice, this approach is most suitable when the population size of individual breeding sites is large enough to avoid inbreeding over the short-term; there are enough breeding sites for different alleles to randomly fix without being lost in the total population; and there is perhaps evidence that the species has evolved in a metapopulation context. In RFS, arguably none of these conditions exist: some populations are very small (e.g. Mayhaw WMA and Garcon Point) and may experience inbreeding over the short

term, reducing survival and reproductive success in an endangered species, if gene flow among breeding sites is kept low. Moreover, very few breeding sites ($n \approx 6$) exist, reducing the likelihood that all alleles will be present in at least one breeding site as they drift to fixation, and increasing the risk that stochastic events could reduce the remaining diversity. Finally, the SNP, MHC, and mitochondrial results obtained here show little population structure and considerable gene flow among Escribano, East Eglin, and West Eglin breeding sites, suggesting that perhaps RFS may not have evolved in a metapopulation scenario. For these reasons, the historic connection among breeding sites should be maintained to facilitate gene flow, thereby reducing genetic drift and inbreeding at individual breeding sites. This is especially crucial given the evident low diversity at immune genes and potential susceptibility to disease (Chapter 1; Williams et al. *in prep*). In the future, managing RFS breeding sites as metapopulations may be a better option if population sizes recover sufficiently to limit inbreeding over the short term, and enough breeding sites have been reestablished to ensure that all alleles are likely to be present in the total population as they become randomly fixed in individual breeding sites.

Together with translocations, repatriations could help to re-establish RFS populations on historically occupied sites, now extirpated (Palis et al. 1997). Recolonization of extirpated sites is unlikely to occur without human help as they are too far from current active sites to naturally re-establish especially because females are less likely to disperse long distances. However, repatriating individuals could begin to expand the limited range of this salamander and ensure their long-term resilience. Raising larvae *in situ* using artificial tanks has been successfully implemented with ambystomatids (Semlitsch and Wilbur 1988, Croshaw and Pechmann 2015) including RFS on Eglin (Fenolio et al. 2014). Raised larvae can be released from tanks into repatriation ponds shortly before they metamorphose, thus optimizing survival during the larval

stage, ensuring sufficient development, and allowing larvae to naturally metamorphose and establish a connection to the new breeding habitat. Translocations and repatriations should optimize genetic diversity by sourcing salamanders from as many breeding sites as possible, not just from the single closest site, given that levels of genetic diversity are low (Chapter 1; Williams et al. *in prep*) and outbreeding depression is unlikely (Frankham et al. 2011). Sites further from the ocean should be prioritized for repatriation in order to minimize the risks posed by hurricanes and associated saltwater intrusion, as well as sea level rise. Also, repatriation sites should be isolated from breeding populations in order to reduce the risk of spreading diseases between current RFS sites. Finally, time is a resource that is also in short supply, increasing frequency of strong hurricanes (Hurricane Michael 2018) and the potential for inbreeding at these sites underlines the need to begin reestablishing RFS populations in order to avoid extinction. Reestablishing extirpated populations and geneflow via human mediated dispersal should be prioritized in order to begin recovering the reticulated flatwoods salamander.

Chapter 4. General Conclusions

The goal of this thesis was to inform the conservation of the reticulated flatwoods salamander (RFS) by measuring genetic diversity at immune genes and assessing population structure as well as migration between extant breeding sites of the RFS using immune genes and mitochondrial DNA. Immune gene diversity was measured through two approaches: first, by Sanger sequencing two major histocompatibility complex (MHC) genes in hundreds of salamanders; then, using a target enrichment experiment to isolate hundreds of immunome SNPs. Low MHC diversity was found as only three MHC class Iα alleles and five MHC class IIβ alleles were discovered. Estimates of population structure within and between breeding sites were low for nuclear markers but showed some structuring with mitochondrial DNA. This is indicative of male biased dispersal and may be evidence of higher philopatry in females, which might be caused by the selective pressures associated with fall breeding. Historic and contemporary migration between sites was high, specifically migration between East Eglin, West Eglin, and Escribano. All three marker types (MHC, SNPs, and mtDNA) provide estimates of migration that support the conclusion that these three populations were connected through gene flow. Ultimately, considerations should be made to reconnect RFS populations through human mediated dispersal, which could increase genetic diversity, reestablish gene flow, and reduce the overall risk of extinction for the reticulated flatwoods salamander.

Literature Cited

Aguilar A, Roemer G, Debenham S, et al. (2004) High MHC diversity maintained by balancing selection in an otherwise genetically monomorphic mammal. Proceedings of the National Academy of Sciences 101:3490–3494.

Alberts B, Johnson A, Lewis J, Raff M, Roberts K, Walter P (2015) Molecular Biology of the Cell, 6th edition. Chapter 24. New York: Garland Science.

Alexander DH, Novembre J, Lange K (2009) Fast model-based estimation of ancestry inunrelated individuals. Genome Research 19:1655–1664.

Allender MC, Bunick D, Mitchell MA (2013) Development and validation of TaqMan quantitative PCR for detection of frog virus 3-like virus in eastern box turtles (*Terrapene carolina carolina*). Journal of Virological Methods 188:121–125.

Allendorf, F. W., Luikart G., Aitken S. (2013) Conservation and the genetics of populations. Blackwell publishing.

Bandelt HJ, Forster P, Rohl A (1999) Median-joining networks for inferring intraspecific phylogenies. Molecular Biology and Evolution 16:37–48.

Bataille A, Cashins SD, Grogan L, et al. (2015) Susceptibility of amphibians to chytridiomycosis is associated with MHC class II conformation. Proceedings of the Royal Society B: Biological Sciences 282:20143127–20143127.

Beerli P, Felsenstein J (1999) Maximum-likelihood estimation of migration rates and effective population numbers in two populations using a coalescent approach. Genetics Society of America 12.

Beerli P, Felsenstein J (2001) Maximum likelihood estimation of a migration matrix and effective population sizes in n subpopulations by using a coalescent approach. Proceedings of the National Academy of Sciences 98:4563–4568.

Benjamini Y, Hochberg Y (1995) Controlling the false discovery rate: a practical and powerful approach to multiple testing. Journal of the Royal Statistical Society. Series B 57:289-300.

Berger L, Speare R, Daszak P, et al. (1998) Chytridiomycosis causes amphibian mortality associated with population declines in the rain forests of Australia and Central America. Proceedings of the National Academy of Sciences 95:9031–9036.

Bernatchez L, Landry C (2003) MHC studies in nonmodel vertebrates: what have we learned about natural selection in 15 years? Journal of evolutionary biology 16:363–377.

Blackburn M, Wayland J, Smith WH, et al. (2015) First report of *ranavirus* and *Batrachochytrium dendrobatidis* in green salamanders (*Aneides aeneus*) from Virginia, USA. Herpetological Review 46:357–361.

Bonin A, Nicole F, Pompanon F, et al. (2007) Population adaptive index: a new method to help measure intraspecific genetic diversity and prioritize populations for conservation. Conservation Biology 21:697–708.

Bos DH, DeWoody JA (2005) Molecular characterization of major histocompatibility complex class II alleles in wild tiger salamanders (*Ambystoma tigrinum*). Immunogenetics 57:775–781.

Brooks GC, Smith JA, Frimpong EA, et al. (2019) Indirect connectivity estimates of amphibian breeding wetlands from spatially explicit occupancy models. Aquatic Conservation: Marine and Freshwater Ecosystems.

Bryant DM, Johnson K, DiTommaso T, et al. (2017) A Tissue-Mapped Axolotl De Novo Transcriptome Enables Identification of Limb Regeneration Factors. Cell Reports 18:762–776.

Burkhart JJ, Peterman WE, Brocato ER, et al. (2017) The influence of breeding phenology on the genetic structure of four pond-breeding salamanders. Ecology and Evolution 7:4670–4681.

Carey C, Alexander MA (2003) Climate change and amphibian declines: is there a link? Diversity and distributions 9:111–121.

Chandler HC, Rypel AL, Jiao Y, et al. (2016) Hindcasting historical breeding conditions for an endangered salamander in ephemeral wetlands of the southeastern USA: Implications of climate change. PLOS ONE.

Chinchar VG (2002) *Ranaviruses* (family Iridoviridae): Emerging cold-blooded killers. Archives of Virology 147:447–470.

Church SA, Kraus JM, Mitchell JC, et al. (2003) Evidence for multiple Pleistocene refugia in the postglacial expansion of the eastern tiger salamander, *Ambystoma tigrinum tigrnum*. Evolution 57:372–383.

Claytor SC, Subramaniam K, Landrau-Giovannetti N, et al. (2017) *Ranavirus* phylogenomics: signatures of recombination and inversions among bullfrog ranaculture isolates. Virology 511:330–343.

Croshaw DA, Pechmann JHK (2015) Size does not matter for male Marbled Salamanders (*Ambystoma opacum*). Canadian Journal of Zoology 93:735–740.

Danecek P, Auton A, Abecasis G, et al. (2011) The variant call format and VCFtools. Bioinformatics 27:2156-2158.

Dool SE, Puechmaille SJ, Kelleher C, et al. (2016) The effects of human-mediated habitat fragmentation on a sedentary woodland-associated species (*Rhinolophus hipposideros*) at its range margin. Acta Chiropterologica 18:377.

Elbers JP, Taylor SS (2015) GO2TR: a gene ontology-based workflow to generate target regions for target enrichment experiments. Conservation Genetics Resources 7:851–857.

Elbers JP, Taylor SS (2016) Major histocompatibility complex polymorphism in reptile conservation. Herpetological Conservation and Biology 11:1–12.

Excoffier L, Laval G, Schneider S (2005) Arlequin (version 3.0): An integrated software package for population genetics data analysis. Evolutionary Bioinformatics.

Farmer AL, Walls SC, Haas C, et al. (2016) A statewide species and habitat assessment for the reticulated flatwoods salamander, frosted flatwoods salamander, and striped newt. Florida Fish and Wildlife Annual Report.

Fenolio DB, Gorman TA, Jones KC, et al. (2014) Rearing the federally endangered reticulated flatwoods salamander, *Ambystoma bishopi*, from eggs through metamorphosis. Herpetological Review 45:62–65.

Foll M, Gaggiotti O (2008) A genome-scan method to identify selected loci appropriate for both dominant and codominant markers: a Bayesian perspective. Genetics 180:977-993.

Fox S, Greer A, Torres-Cervantes R, Collins J (2006) First case of *ranavirus*-associated morbidity and mortality in natural populations of the South American frog *Atelognathus patagonicus*. Diseases of Aquatic Organisms 72:87–92.

Frankham R, Ballou JD, Briscoe DA (2002) Introduction to conservation genetics. Cambridge University Press.

Frankham R, Ballou JD, Eldridge MDB, et al. (2011) Predicting the probability of outbreeding depression: Predicting outbreeding depression. Conservation Biology 25:465–475.

Frost CC (1993) Four centuries of changing landscape patterns in the longleaf pine ecosystem. In: Proceedings of the Tall Timbers fire ecology conference. pp 17–43.

Fu M, Waldman B (2017) Major histocompatibility complex variation and the evolution of resistance to amphibian chytridiomycosis. Immunogenetics 69:529–536.

Gorman TA, Haas CA, Himes JG (2013) Evaluating methods to restore amphibian habitat in fire-suppressed pine flatwoods wetlands. Fire Ecology 9:96–109.

Goudet J (2005) HIERFSTAT, a package for R to compute and test hierarchical F-statistics. Molecular Ecology Notes 5:184-186.

Goudet, J (2001) FSTAT, a program to estimate and test gene diversities and fixation indices (version 2.9.3). http://www2.unil.ch/popgen/softwares/fstat.htm.

Grant E, Miller D, Schmidt B, et al. (2016) Quantitative evidence for the effects of multiple drivers on continental-scale amphibian declines. Scientific Reports 6

Gray MJ, Chinchar VG (eds) (2015) *Ranaviruses*. Springer International Publishing, Cham, Switzerland.

Greer A, Brunner J, Collins J (2009) Spatial and temporal patterns of ambystoma tigrinum virus (ATV) prevalence in tiger salamanders *Ambystoma tigrinum nebulosum*. Diseases of Aquatic Organisms 85:1–6.

Helfer V, Broquet T, Fumagalli L (2012) Sex-specific estimates of dispersal show female philopatry and male dispersal in a promiscuous amphibian, the alpine salamander (*Salamandra atra*). Molecular Ecology 21:4706–4720.

IUCN (2013) Guidelines for Reintroductions and Other Conservation Translocations. Version 1.0. Gland, Switzerland: IUCN Species Survival Commission, viiii.

IUCN [International Union for Conservation of Nature] (2008) *Ambystoma bishopi*: John Palis, Geoffrey Hammerson: The IUCN red list of threatened species. International Union for Conservation of Nature.

Johnson AJ, Pessier AP, Wellehan JFX, et al. (2008) *Ranavirus* infection of free-ranging and captive box turtles and tortoises in the United States. Journal of Wildlife Diseases 44:851–863.

Kearse M, Moir R, Wilson A, et al. (2012) Geneious Basic: an integrated and extendable desktop software platform for the organization and analysis of sequence data. Bioinformatics 28:1647-1649.

Kiemnec-Tyburczy KM, Richmond JQ, Savage AE, et al. (2012) Genetic diversity of MHC class I loci in six non-model frogs is shaped by positive selection and gene duplication. Heredity 109:146

Kik M, Martel A, Sluijs AS der, et al. (2011) *Ranavirus*-associated mass mortality in wild amphibians, The Netherlands, 2010: A first report. The Veterinary Journal 190:284–286.

Kosch TA, Eimes JA, Didinger C, et al. (2017) Characterization of MHC class IA in the endangered southern corroboree frog. Immunogenetics 69:165–174.

Kraus BT, McCallen EB, Williams RN (2017) Evaluating the Survival of Translocated Adult and Captive-reared, Juvenile Eastern Hellbenders (*Cryptobranchus alleganiensis alleganiensis*). Herpetologica 73:271–276.

Kumar S, Stecher G, Li M, Knyaz C, Tamura K (2018) MEGA X: Molecular Evolutionary Genetics Analysis across computing platforms. Molecular Biology and Evolution 35:1547-1549.

Li H, Handsaker B, Wysoker A, et al. (2009) The Sequence Alignment/Map format and SAMtools. Bioinformatics 25:2078-2079.

Liebgold EB, Brodie ED, Cabe PR (2011) Female philopatry and male-biased dispersal in a direct-developing salamander, *Plethodon cinereus*. Molecular Ecology 20:249–257.

Lischer H, Excoffier L (2012) PGDSpider: an automated data conversion tool for connecting population genetics and genomics programs. Bioinformatics 28:298-299.

Mao J, Hedrick RP, Chinchar VG (1997) Molecular characterization, sequence analysis, and taxonomic position of newly isolated fish iridoviruses. Virology 229:212–220.

Marsh IB, Whittington RJ, O'Rourke B, et al. (2002) Rapid differentiation of Australian, European and American *ranaviruses* based on variation in major capsid protein gene sequence. Molecular and Cellular Probes 16:137–151.

Martel A, Spitzen-van der Sluijs A, Blooi M, et al. (2013) *Batrachochytrium salamandrivorans* sp. nov. causes lethal chytridiomycosis in amphibians. Proceedings of the National Academy of Sciences 110:15325–15329.

McCallen EB, Kraus BT, Burgmeier NG, et al. (2018) Movement and Habitat Use of Eastern Hellbenders (*Cryptobranchus alleganiensis alleganiensis*) Following Population Augmentation. 11.

McCallum ML (2007) Amphibian decline or extinction? Current declines dwarf background extinction rate. Journal of Herpetology 41:483–491.

McCartney-Melstad E, Vu JK, Shaffer HB (2018) Genomic data recover previously undetectable fragmentation effects in an endangered amphibian. Molecular Ecology 27:4430–4443.

McIntyre RK, Guldin JM, Ettel T, et al. (2018) Restoration of longleaf pine in the southern United States: A status report. 6

Miller D, Gray M, Storfer A (2011) Ecopathology of *ranaviruses* infecting amphibians. Viruses 3:2351–2373.

Moore MP, Whiteman HH (2016) Natal philopatry varies with larval condition in salamanders. Behavioral Ecology and Sociobiology 70:1247–1255.

O'Donnell KM, Messerman AF, Barichivich WJ, et al. (2017) Structured decision making as a conservation tool for recovery planning of two endangered salamanders. Journal for Nature Conservation 37:66–72.

O'Hanlon SJ, Rieux A, Farrer RA, et al. (2018) Recent Asian origin of chytrid fungi causing global amphibian declines. Science 360:621–627.

Ortutay C, Vihinen M (2006) Immunome: a reference set of genes and proteins for systems biology of the human immune system. Cellular Immunology 244:87-89.

Palis J (1996) Flatwoods salamander (*Ambystoma cingulatum* Cope). Natural Areas Journal 16:49–54.

Palis JG (1997) Breeding migration of *Ambystoma cingulatum* in Florida. Journal of Herpetology 31:71.

Pauly GB, Piskurek O, Shaffer HB (2007) Phylogeographic concordance in the southeastern United States: The flatwoods salamander, *Ambystoma cingulatum*, as a test case: flatwoods salamander phylogeography. Molecular Ecology 16:415–429.

Peterman WE, Anderson TL, Ousterhout BH, et al. (2015) Differential dispersal shapes population structure and patterns of genetic differentiation in two sympatric pond breeding salamanders. Conservation Genetics 16:59–69.

Petranka J (2010) Salamanders of the United States and Canada. Washington, Smithsonian Institution Press.

Picco AM, Brunner JL, Collins JP (2007) Susceptibility of the endangered California tiger salamander, *Ambystoma californiense*, to *ranavirus* infection. Journal of wildlife diseases 43:286–290

Price SJ, Garner TWJ, Nichols RA, et al. (2014) Collapse of amphibian communities due to an introduced *ranavirus*. Current Biology 24:2586–2591.

Pritchard JK, Stephens M, Donnelly P (2000) Inference of population structure using multilocus genotype data. Genetics Society of America 15.

R Core Team (2018) R: A language and environment for statistical computing. R Foundation for Statistical Computing, Vienna, Austria.

Raj A, Stephens M, Pritchard JK (2014) fastSTRUCTURE: Variational inference of population structure in large SNP data sets. Genetics 197:573-589.

Raymond M, Rousset F, (1995) GENEPOP (version 1.2): population genetics software for exact tests and ecumenicism. Journal of Heredity, 86:248-249.

Richman AD, Herrera G, Reynoso VH, et al. (2007) Evidence for balancing selection at the DAB locus in the axolotl, *Ambystoma mexicanum*. International Journal of Immunogenetics 34:475–478.

Richmond JQ, Savage AE, Zamudio KR, Rosenblum EB (2009) Toward immunogenetic studies of amphibian chytridiomycosis: Linking innate and acquired immunity. BioScience 59:311–320.

Rittmeyer EN, Austin CC (2015) Combined next-generation sequencing and morphology reveal fine-scale speciation in Crocodile Skinks (Squamata: Scincidae: Tribolonotus). Molecular Ecology 24:466–483

Rousset F, (2008) Genepop'007: a complete reimplementation of the Genepop software for Windows and Linux. Molecular Ecology Resources 8: 103-106.

Rozas J, Ferrer-Mata A, Sánchez-DelBarrio JC, et al. (2017). DnaSP 6: DNA sequence polymorphism analysis of large datasets. Molecular Biology and Evolution 34: 3299-3302.

Sacerdote AB (2009) Reintroduction of extripated flatwoods amphibians into restored forested wetlands in northern Illinois: feasibility, assessment, implimentation, habitat restoration and conservation implications (PhD dissertation). Norther Illinois University, DeKalb, IL

Sammut B, Du Pasquier L, Ducoroy P, et al. (1999) Axolotl MHC architecture and polymorphism. European Journal of Immunology 29:2897–2907.

Sammut B, Laurens V, Tournefier A (1997) Isolation of MHC class I cDNAs from the axolotl *Ambystoma mexicanum*. Immunogenetics 45:285–294.

Savage AE, Mulder KP, Torres T, Wells S (2018) Lost but not forgotten: MHC genotypes predict overwinter survival despite depauperate MHC diversity in a declining frog. Conservation Genetics 19:309–322.

Savage AE, Muletz-Wolz CR, Campbell Grant EH, et al. (2019) Functional variation at an expressed MHC class IIβ locus associates with *ranavirus* infection intensity in larval anuran populations. Immunogenetics 71:335–346.

Savage AE, Terrell KA, Gratwicke B, et al. (2016) Reduced immune function predicts disease susceptibility in frogs infected with a deadly fungal pathogen. Conservation Physiology.

Savage AE, Zamudio KR (2011) MHC genotypes associate with resistance to a frog-killing fungus. Proceedings of the National Academy of Sciences 108:16705–16710.

Savage AE, Zamudio KR (2016) Adaptive tolerance to a pathogenic fungus drives major histocompatibility complex evolution in natural amphibian populations. Proceedings of the Royal Society B: Biological Sciences 283:20153115.

Semlitsch RD, Walls SC, Barichivich WJ, O'Donnell KM (2017) Extinction debt as a driver of amphibian declines: An example with imperiled flatwoods salamanders. Journal of Herpetology 51:12–18.

Semlitsch RD, Wilbur HM (1988) Effects of Pond Drying Time on Metamorphosis and Survival in the Salamander (*Ambystoma talpoideum*). Copeia 1988:978.

Shaffer HB, McKnight ML (1996) The polytypic species revisited: Genetic differentiation and molecular phylogenetics of the tiger salamander *Ambystoma tigirnum* (Amphibia: Caudata) complex. Evolution 50:417–433.

Sommer, Simone (2005) The Importance of Immune Gene Variability (MHC) in Evolutionary Ecology and Conservation. Frontiers in Zoology 2:16-34.

Sommer, Simone, Allan D. McDevitt, and Niko Balkenhol (2013) Landscape Genetic Approaches in Conservation Biology and Management. Conservation Genetics 14:249-51.

Taylor SS, Jenkins DA, Arcese P (2012) Loss of MHC and neutral variation in Peary Caribou: Genetic drift is not mitigated by balancing selection or exacerbated by MHC allele distributions. PLoS ONE.

Teacher AGF, Garner TWJ, Nichols RA (2009) Evidence for directional selection at a novel major histocompatibility class I marker in wild common frogs (*Rana temporaria*) exposed to a viral pathogen (*ranavirus*). PLoS ONE.

Tracy KE, Kiemnec-Tyburczy KM, DeWoody JA, et al. (2015) Positive selection drives the evolution of a major histocompatibility complex gene in an endangered Mexican salamander species complex. Immunogenetics 67:323–335.

USFWS [U.S. Fish and Wildlife Service] (2015) Reticulated flatwoods salamander (*Ambystoma bishopi*) 5-Year review: Summary and evaluation. Federal Register. 79 FR 56821.

Wang IJ, Shaffer HB (2017) Population genetic and field-ecological analyses return similar estimates of dispersal over space and time in an endangered amphibian. Evolutionary Applications 10:630–639.

Waples RS (2015) Testing for Hardy–Weinberg Proportions: Have We Lost the Plot? Journal of Heredity 106:1–19.

Weir B, Cockerham C (1984) Estimating F-Statistics for the Analysis of Population Structure. Evolution, 38:1358-1370

Weir BS, Cockerham CC (1984) Estimating F-statistics for the analysis of population structure. Evolution 38:1358–1370.

Wendt AS, (2017) A population genetic investigation of the reticulated flatwoods salamander (*Ambystoma bishopi*) on Eglin Air Force Base (MS thesis). Georgia Southern University, Statesboro, GA.

Whiteley, AR, McGarigal K, and Schwartz MK (2014) Pronounced differences in genetic structure despite overall ecological similarity for two Ambystoma salamanders in the same landscape. Conservation Genetics 15:573–91.

Williams ST, Haas C, Roberts J, et al. (*in prep*) Depauperate major histocompatibility complex variation in the endangered reticulated flatwoods salamander (*Ambystoma bishopi*).

Wilson GA, Rannala B (2003) Bayesian inference of recent migration rates using multilocus genotypes. Genetics Society of America 16

Zamudio KR, Savage WK (2003) Historical isolation, range expansion, and secondary contact of two highly divergent mitochondrial lineages in spotted salamanders (*Ambystoma maculatum*). Evolution 57:1631–1652.

Zhao M, Wang Y, Shen H, et al. (2013) Evolution by selection, recombination, and gene duplication in MHC class I genes of two Rhacophoridae species. BMC Evolutionary Biology 13:113.

Zhu R, Chen Z, Wang J, et al. (2014) Extensive diversification of MHC in Chinese giant salamanders *Andrias davidianus* (Anda-MHC) reveals novel splice variants. Developmental & Comparative Immunology 42:311–322.

Vita

Steven Tyler Williams was born in Roanoke, Virginia and lived in Franklin county Virginia throughout grade school. He attended Virginia Tech from 2009 - 2012, where he pursued a Bachelor of Science in Wildlife Biology. Upon graduation Tyler went to work for the United States Geological Service and then on to a project with reticulated flatwoods salamanders on Eglin Air-force Base, Florida. After working three salamander breeding seasons on the Air-force Base Tyler went to work with Dr. Sabrina Taylor as a research assistant at Louisiana State University. In the fall of 2017, after two years as a research associate, he began working with Dr. Taylor on a project that combined conservation genetics and the reticulated flatwoods salamander. The goal of his project was to measure immune gene diversity and population structure in the reticulated flatwoods salamander, a species which has had little genetic research conducted to date. Tyler plans to finish his MS in 2019 after studying conservation genetics and the reticulated flatwoods salamander for two years. He will go on to work for the United States Department of Agriculture at the honeybee breeding and genomics facility in Baton Rouge, Louisiana.